Atmos. Chem. Phys. Discuss., 13, 7811–7869, 2013
www.atmos-chem-phys-discuss.net/13/7811/2013/
doi:10.5194/acpd-13-7811-2013

Atmospheric Chemistry and Physics Discussions
Open Access

Contact freezing: a review

L. A. Ladino[1,*], O. Stetzer[1], and U. Lohmann[1]

[1]Institute for Atmospheric and Climate Science, ETH Zurich, Universitätstrasse 16, 8092 Zurich, Switzerland
[*]now at: Department of Chemistry, University of Toronto, Toronto, Ontario, Canada

Received: 8 March 2013 – Accepted: 11 March 2013 – Published: 21 March 2013

Correspondence to: L. A. Ladino (lladino@chem.utoronto.ca)

Published by Copernicus Publications on behalf of the European Geosciences Union.

Abstract

This manuscript compiles both theoretical and experimental information on contact freezing with the aim to better understand this potentially important but still not well quantified heterogeneous freezing mode. There is no complete theory that describes contact freezing and how the energy barrier has to be overcome to nucleate an ice crystal by contact freezing. Experiments on contact freezing indicate that it can initiate ice formation at the highest temperatures. A difference in the freezing temperatures between contact and immersion freezing has been found using different instrumentation and different ice nuclei. There is a lack of data on collision rates in most of the reported data, which inhibits a quantitative calculation of the freezing efficiencies. Thus, new or modified instrumentation to study this heterogeneous freezing mode in the laboratory and in the field are needed. Important questions concerning contact freezing and its potential role for ice cloud formation and climate are also summarized.

1 Introduction

Clouds play an important role in the global radiative budget (Trenberth et al., 2009) as they cover around 70 % of the Earth's surface (Stubenrauch et al., 2010). Depending on cloud type, clouds can either cool and/or heat the Earth's surface. Clouds can reflect shortwave (solar) radiation cooling the Earth or they can absorb and re-emit long wave radiation emitted by the Earth's surface back towards the surface causing a warming. Aerosol particles can act as cloud condensation nuclei (CCN), and a much smaller fraction of atmospheric aerosol particles acts as heterogeneous ice nuclei (IN) to catalyze ice formation below 0 °C. Thus, aerosol particles are important in cloud formation (e.g. lifetime, droplet size, cloud phase and cloud albedo) and therefore influence the hydrological cycle (Lohmann and Feichter, 2005). Most of the precipitation in mid-latitudes originates via the ice phase but reaches the surface as rain (melting of ice crystals) (Lau and Wu, 2003; Lohmann and Feichter, 2005; Lohmann and

ACPD
13, 7811–7869, 2013

Diehl, 2006). IN are mostly solid aerosol particles, either insoluble or crystalline. IN are thought to have a similar crystalline structure to ice and/or the possibility to form hydrogen bonds and to possess active sites (i.e. crevasses, imperfections, corners and/or steps onto the particle surface). Possible physical and chemical influences are summarized in Pruppacher and Klett (1997) and Vali (1999) (e.g. water uptake, particle morphology, hygroscopicity and presence of ions between the particle layers). Natural aerosol particles such as bioaerosols (e.g. bacteria, pollen and fungi), volcanic ash and soil particles (e.g. mineral dust and clays) have been found to be good IN. Organic aerosols, such as citric acid, levoglucosan and raffinose (Murray et al., 2010; Wang et al., 2012; Wagner et al., 2012); and crystalline particles, such as ammonium sulfate (Abbatt et al., 2006) or hydrated sodium chloride (Wise et al., 2012) may also serve as IN. Artificial particles such as silver iodide (AgI) have been used in the laboratory and in cloud seeding studies (Wieringa and Holleman, 2006) because they were found to be good IN. Diehl and Mitra (1998) and Gorbunov et al. (2001) found that soot particles can also act as IN, whereas other studies suggest that this is not always the case (DeMott, 1990; Möhler et al., 2005; Dymarska et al., 2006; Friedman et al., 2011; Hoose and Möhler, 2012). Therefore, predicting the IN activity, if any, of atmospheric soot is limited by poor current understanding.

To understand ice formation in mixed-phase clouds, it is crucial to study each of the four known heterogeneous ice nucleation modes (deposition nucleation, condensation freezing, immersion freezing and contact freezing) in detail. The preference of one freezing mechanism over another depends on IN composition, temperature and supersaturation with respect to ice and/or water and the presence of liquid supercooled droplets. Deposition nucleation occurs when water vapor deposits onto an IN. In contrast, condensation freezing occurs when water vapor condenses around the particle at temperatures below 0 °C to form a supercooled liquid droplet which subsequently freezes. Immersion freezing takes place when an IN is immersed within a liquid droplet at temperatures where it does not freeze, thereafter the liquid droplet is cooled down and initiates ice formation. The last heterogeneous freezing mode is contact freezing.

ACPD
13, 7811–7869, 2013

Rau (1950); Fletcher (1969, 1970); Cooper (1974) and Fukuta (1975) presented some of the first ideas on the concept of contact freezing. They defined it as the process in which freezing of a supercooled droplet results from the collision with an aerosol particle (Vali (1985) and definitions by the International Commission on Clouds and Precipitation (ICCP) and the International committee on Nucleation and Atmospheric Aerosols (ICNAA)). Ice formation can be enhanced by contact freezing within mixed-phase clouds since both aerosol particles and supercooled cloud droplets may be present. Inside these clouds, the interstitial aerosol particles collide with the supercooled liquid droplets by different physical forces such as Brownian motion, inertial impaction, interception, electroscavenging, thermophoresis and diffusiophoresis (Greenfield, 1957; Slinn and Hales, 1971; Beard, 1974; Wang et al., 1978).

In the past, a lot of work has been done to study the conditions relevant for the different heterogeneous modes of ice formation. Here we only discuss studies of contact and immersion freezing with which contact freezing will be compared. These two freezing modes are frequently compared; however, this comparison is not very trivial and requires more attention. Several experiments on immersion freezing using different instrumentation (e.g. the cold plate (Shaw et al., 2005; Vali, 2008), the Differential Scanning Calorimeter (DSC, Marcolli et al., 2007), the wind tunnel (Pitter and Pruppacher, 1973; Diehl et al., 2002; Von Blohn et al., 2005), the Immersion Mode Cooling Chamber (IMCA, Lüönd et al., 2010) and the Leipzig Aerosol Cloud Interaction Simulator (LACIS, Niedermeier et al., 2010)) and different aerosol particles have been reported.

Since 1973 several research groups studied contact freezing using different instrumentation such as cloud chambers (e.g. the NCAR ice nucleation counter (Langer et al., 1978), the thermal diffusion chamber (Schaller and Fukuta, 1979), the isothermal cloud chamber (ICC, DeMott et al., 1983; DeMott, 1995) and the CoLlision Ice Nucleation CHamber (CLINCH, Ladino et al., 2011b)), a wind tunnel (Pitter and Pruppacher, 1973; Levin and Yankofsky, 1983; Diehl and Mitra, 1998; Diehl et al., 2002; Von Blohn et al., 2005), a cold plate (Fukuta, 1975; Rosinski and Nagamoto, 1976; Durant and Shaw, 2005; Shaw et al., 2005) and a ElectroDynamic Balance (EDB, Svensson et al.,

ACPD
13, 7811–7869, 2013

2009). The collisions of the aerosol particles with droplets have been simulated in different ways. For example, Shaw et al. (2005); Durant and Shaw (2005) and Fornea et al. (2009) performed their experiments using a cold plate where the aerosol particles were brought into contact with the drops mechanically. In contrast, in the wind tunnel (e.g. Pitter and Pruppacher, 1973; Levin and Yankofsky, 1983; Diehl and Mitra, 1998; Von Blohn et al., 2005), EDB (Svensson et al., 2009) and cloud chamber studies (e.g. Langer et al., 1978; DeMott et al., 1983; DeMott, 1995; Ladino et al., 2011b) the aerosol particles were naturally scavenged from air by the liquid drops.

Several detailed reviews on ice nucleation have been published (e.g. Mossop, 1963; Vali, 1985; Pruppacher and Klett, 1997; Hoose and Möhler, 2012; Murray et al., 2012). The ice nuclei concentrations, freezing pathways, proposed mechanisms and hypotheses to explain the observations have been revised. However, there is no paper that compiles the available information on contact freezing which is believed to initiate ice at the highest temperatures (e.g. Hoose and Möhler, 2012). The high freezing onset temperature due to contact nucleation could be partially attributed to scavenging processes because for instance thermophoresis attracts IN to evaporating droplets (see Sect. 2.1). Larger aerosol particles and higher aerosol concentrations are expected at low altitudes and at the cloud base where higher temperatures are experienced.

If the laboratory observations are representative for atmospheric conditions, contact freezing could be responsible for ice formation in clouds at earlier development stages (i.e. higher temperatures). There are only few attempts to measure contact freezing nuclei concentrations in natural air (Deshler and Vali, 1992; Meyers et al., 1992). These field measurement are highly valuable since they are useful to validate the laboratory observations before they could be accurately implemented in climate models. Changes in the numbers of contact freezing nuclei will impact the indirect effect of the aerosol particles causing more precipitation and less reflection of solar radiation back to space (Lohmann, 2002).

Hoose et al. (2010) developed a parameterization to calculate the contact freezing nucleation rates with the aim to investigate the importance of this freezing mode in

ACPD
13, 7811–7869, 2013

global climate models and hence on climate. The obtained rates for soot particles are comparable to that of soot in the immersion freezing mode. However, the rates for dust particles are lower than the corresponding values in the deposition nucleation and immersion freezing modes because of the large size of dust particles that renders collisions less likely than in the case of soot. It can be deduced that contact freezing could play an important role in cloud formation (even though it is not the dominant pathway to form ice globally) since it can directly compete with the other nucleation modes to nucleate ice.

In this manuscript we summarize the available theories, instrumentation and experimental studies on contact freezing with a special focus on the experimental results and instrumentation. We highlight uncertainties of previous experiments and suggest possible modifications in future experiments in order to increase their usefulness for the scientific community. The limitations of the currently available instrumentation are provided with the aim to build new and better instruments to study contact freezing in the future.

Answering the following key questions will help us to understand the role of contact freezing in cloud formation and climate. Some of these points were already highlighted by Vali (1985) and Meyers et al. (1992) but they remain open and/or uncertain:

- Which is the most appropriate or realistic theory to explain ice formation due to contact freezing from a microscopic perspective?
- Is the collision energy crucial to initiate freezing or is it purely an air-water interphase effect?
- Is contact freezing time dependent and thus a stochastic process?
- Does the particle stick on the droplet surface as found by Gokhale and Goold Jr. (1968) or does the particle get partially or completely immersed into the droplet? If the latter, what are the particle penetration rates?

ACPD
13, 7811–7869, 2013

- How many collisions are needed to trigger the freezing of cloud droplets due to contact freezing? What are the freezing efficiencies of different IN's in contact freezing mode?
- Do parameters other than particle type, aerosol size, temperature, aerosol particle concentration and time influence contact freezing? Does droplet size matter?
- Why is contact freezing more efficient to nucleate ice than the other freezing modes?
- Is contact freezing an especially effective mechanism also in real atmospheric cloud situations?

2 Theory behind contact freezing

The difficulty to experimentally study contact freezing as well as to describe it theoretically results from the fact that contact freezing is a combination of two processes: the collision between supercooled droplets and aerosol particles, and the initiation of freezing due to both being or getting in contact with each other. The challenge is to de-convolve these two processes and describe them independently.

2.1 Collision efficiency

Collision efficiency (CE) describes the fraction of aerosol particles in the sweep-out volume that effectively get in contact with a droplet, falling by its terminal velocity. Figure 1 shows a schematic of how aerosol particles can collide with sedimenting water droplets due to different forces.

The aerosol particles within the sweep-out volume can be moved towards or away from the cloud droplets by the air molecules due to their random movements. This effect termed Brownian motion is most important for small aerosol particles (aerosol particles (a) smaller than $\approx 0.1\,\mu m$ in radius). The smaller the particles, the larger the

ACPD
13, 7811–7869, 2013

Brownian motion effect. When the aerosol particle radii are larger than ≈ 0.5 µm, their inertia are large enough to deviate from the trajectories of the surrounding air and impact onto the cloud droplets. Interception occurs when particles are of sizes that enable them to follow the parcel trajectories around the droplet but end up in the droplet boundary layer, very close to its surface where they are "intercepted" by the droplet. Interception is important in the same particle size range as inertial impaction. If electrical charges are present both on the aerosol particles and droplets, the aerosol particles can be attracted by the charges on the droplet. The phoretic forces (thermophoresis and diffusiophoresis) take place when cloud droplets are evaporating or growing by condensation. During evaporation or growth by condensation a temperature gradient between the droplet and its surrounding is created. Air molecules at the warmer side have a higher kinetic energy and thus exert a net force on the particles towards the colder temperature (thermophoresis). At the same time, a water vapor gradient (diffusiophoresis) is generated in the opposite direction which moves the aerosol particles in the opposite direction as thermophoresis. Electroscavenging and the phoretic forces are important in the "Greenfield gap", i.e. at the transition regime between Brownian motion and inertial impaction (aerosol particles from ≈ 0.1 µm to ≈ 1.0 µm in radius).

Several experimental (e.g. Beard, 1974; Lai et al., 1978; Leong et al., 1982; Deshler, 1985; Pranesha and Kamra, 1996; Vohl et al., 2001; Ladino et al., 2011a) and theoretical (e.g. Greenfield, 1957; Slinn and Hales, 1971; Isaac and Douglas, 1972; Wang et al., 1978; Herbert and Beheng, 1986; Tinsley et al., 2001; Park et al., 2005; Andronache et al., 2006; Croft et al., 2009) studies have been conducted to quantify the efficiency at which cloud drops and aerosol particles collide as a function of particle size and concentration, droplet size, relative humidity (RH_w) and electric fields. Most of the parameterizations and/or models to determine the collision rates were developed for conditions below cloud with the exception of the Isaac and Douglas (1972), the Young (1974a) and the Wang et al. (1978) models.

Figure 2 shows the collision efficiency as a function of particle size and RH_w using a combination of Wang et al. (1978)'s, Park et al. (2005)'s and Andronache et al.

ACPD
13, 7811–7869, 2013

(2006)'s models as an illustration. Although Wang et al. (1978) assumed the simultaneous action of the dynamical forces, with only the net force acting on the particle; Park et al. (2005) and Andronache et al. (2006) assumed different forces to act independently. Therefore, they added the single forces to determine the total CE.

Some experimentalists rely on collision efficiency models because the experimental determination of the collision efficiency is very difficult if not impossible.

2.2 Freezing efficiency

The freezing efficiency describes the average number of collisions of particles with supercooled droplets which are required to freeze one droplet by contact freezing. In other words the freezing efficiency is the freezing probability per droplet-particle collision. It is a function of temperature and sums up the particle properties influencing the freezing process in that mode.

Knowing the collision efficiencies with the particle's terminal velocity (v_t) and the aerosol number concentration (N_a), the number of particles (N_{coll}), which effectively collide with the droplet, can be calculated as follows:

$$N_{coll}(t) = \int \pi \cdot (r(t) + a)^2 \cdot CE \cdot v_t(t) \cdot N_a dt. \quad (1)$$

For a given residence time (t) of a droplet (r) in an environment with a constant temperature and aerosol concentration, an experimental frozen fraction (FF) can be measured. Equation (1) relates to one droplet. To derive a frozen fraction it is necessary to average over many observations of individual droplets.

$$FF(t) = \frac{N_{frozen}}{N_{total}}, \quad (2)$$

ACPD
13, 7811–7869, 2013

where N_{frozen} is the number of frozen droplets and N_{total} is the total number of studied droplets (liquid + ice). Hence, the freezing efficiency FE, can be defined as follows:

$$FE = \frac{FF(t)}{N_{coll}(t)} = \frac{N_{frozen}}{N_{total}} \frac{1}{\int \pi \cdot (r(t) + a)^2 \cdot CE \cdot v_t(t) \cdot N_a dt}. \quad (3)$$

2.3 Theories about contact freezing

Pruppacher and Klett (1997) summarized the theories which were available in the 1970s. They focused on active sites (e.g. Fletcher, 1969) as the main difference between contact freezing and the other heterogeneous freezing modes. Later on, Tabazadeh et al. (2002), Djikaev et al. (2002) and Djikaev and Ruckenstein (2008) explained the differences between different heterogeneous modes based on a thermodynamical model. The most plausible theories/hypothesis are briefly summarized below.

2.3.1 IN solubility

Fletcher (1970) and Guenadiev (1970) suggested that the solubility of the IN could explain the difference between immersion and contact freezing. It is believed that the ice germ forms on an active site of the IN. Therefore, if the active site characteristics are changed or partially modified it could have consequences for the IN abilities. It is believed that most IN begin as dry and insoluble particles. If a partial soluble IN is immersed in a liquid droplet its surface can be eroded by the surrounding water molecules. As the active sites are located on the IN surface, they can be partially destroyed and/or their size reduced. This causes an IN deactivation or a decrease in the IN ability compared to an IN that collides with a cloud droplet from the outside and initiates freezing immediately.

ACPD
13, 7811–7869, 2013

2.3.2 Ice embryo formation and its size

Cooper (1974) was the first to explain contact freezing theoretically based on the classical nucleation theory. He proposed a possible mechanism for this ice formation pathway. Figure 3 shows a schematic from Cooper (1974) where an ice germ forms on an IN due to deposition nucleation, immersion freezing and contact freezing. He proposed that a sub-critical (deposition nucleation) germ forms on the IN from the vapor phase. Upon contact with a supercooled droplet, freezing is triggered because the same ice embryo is supercritical when surrounded by water (immersion freezing). He assumes that the contact angle in both deposition nucleation and contact freezing is similar because the ice germ forms from the vapor phase. However, the critical ice embryo is larger for deposition nucleation than for contact nucleation which leads to a clear difference in the freezing (i.e. temperature) threshold between these modes. This is illustrated in Fig. 3 by the size of the shaded areas. Hoose et al. (2010) defined the ice embryo radius for deposition nucleation ($r_{g,dep}$, Eq. 4) and immersion freezing ($r_{g,imm}$, Eq. 5) based on Cooper (1974) and Chen et al. (2008).

$$r_{g,dep} = \frac{2 v_w \sigma_{i/v}}{kT \cdot \ln(e/e_{si})}, \quad (4)$$

$$r_{g,imm} = \frac{2 v_w \sigma_{i/w}}{kT \cdot \ln(a_w e_{sw}/e_{si})}, \quad (5)$$

where v_w is the volume of a water molecule in ice, $\sigma_{i/v}$ the surface tension between ice and vapor, $\sigma_{i/w}$ surface tension between ice and water, k the Boltzmann constant, T the temperature, e the water vapor pressure, e_{si} the saturation vapor pressure over ice, a_w the water activity, and e_{sw} the saturation vapor pressure over water.

The critical ice embryo size for contact freezing ($r_{g,con}$) must be formed in the vapor phase and it should be equal or larger than $r_{g,imm}$ in order to nucleate ice upon collision with a supercooled droplet. Besides the critical ice embryo sizes, Cooper (1974) also developed a mathematical expression to calculate the number of contact ice germs per

ACPD
13, 7811–7869, 2013

aerosol particle ($N_{g,contact}$). Cooper's ideas are reflected in Eq. (6) which is a modification from his original work (Hoose et al., 2010).

$$N_{g,contact} = 4\pi r_N^2 \frac{e}{v_s \sqrt{2\pi m_w kT}} \times \exp\left[-\frac{\Delta g^{\#}_{dep} + f\,\Delta g^{\circ}_{g,dep}(r_{g,imm})}{kT}\right], \quad (6)$$

where r_N is the radius of the nucleus, v_s the frequency of vibration of water vapor molecules adsorbed on the solid substrate, m_w the mass of a water molecule, $\Delta g^{\#}_{dep}$ the activation energy for deposition nucleation, f the form factor, and $\Delta g^{\circ}_{g,dep}$ the homogeneous energy for germ formation in the vapor phase.

The threshold difference was validated experimentally (e.g. Pitter and Pruppacher, 1973; DeMott, 1995; Diehl et al., 2001); however, discrepancies using AgI (similar nucleation thresholds for deposition nucleation and contact freezing (Pruppacher and Klett, 1997, p. 339), and soot particles (soot particles were found to be better IN in the immersion freezing mode than in the contact freezing mode Diehl and Mitra, 1998) could not support this theory. Moreover, the available water vapor density in the vicinity of the droplet assumed by Cooper (1974) is not correct as discussed by Pruppacher and Klett (1997).

2.3.3 Mechanical disturbances

Fukuta (1975) tried to explain the difference in freezing temperatures between immersion and contact freezing as a consequence of the water-air interface movement on the IN. Water molecules adsorb on the dry IN surface forming a layer of a variable thickness. The formed water clusters do not reach the critical size to form an ice embryo if the IN is brought in contact with a supercooled droplet until an external energy source is provided to the system. This needed energy is applied to the system (air-water-IN) by the collision between the IN and the droplet. The free energy of the embryo formation

ACPD
13, 7811–7869, 2013

(ΔG^*) and hence the J_{contact} can be determined using Eqs. (7) and (8), respectively.

$$\Delta G^* = \Delta\mu \cdot V + A_{\text{CS}}(\gamma_{\text{CS}} - \gamma_{\text{CL}}) + A_{\text{SL}} \cdot \gamma_{\text{SL}}, \quad (7)$$

$$J_{\text{contact}} = K \cdot \exp\left[\frac{-\Delta G^*}{kT}\right], \quad (8)$$

where $\Delta\mu$ in the free energy difference between ice and water, V the volume of the ice germ, A_{CS} the area between the IN and ice embryo boundary, γ_{CS} surface-free energy between the IN and ice embryo interface, γ_{CL} surface-free energy between the IN and liquid interface, A_{SL} the area between the liquid and the ice embryo boundary, γ_{SL} surface-free energy between the liquid and the ice embryo interface, and K the kinetic constant.

2.3.4 Three-phase contact

A model has been developed to explain the contact freezing mechanism based on thermodynamics (Djikaev and Ruckenstein, 2008). In this model four different phases are taken into account as shown in Fig. 4. The different phases are the liquid and vapor phase, the ice crystal and the foreign particle which are symbolized with α, β, γ and δ, respectively. The needed reversible work to nucleate an ice crystal at the double inter-phase α-δ (immersion freezing) was calculated and compared with the corresponding values at the triple inter-phase α-β-δ (contact freezing). Djikaev and Ruckenstein (2008) found that the required reversible work is smaller if the ice germ forms at the triple inter-phase, i.e. when the IN is located at the droplet surface. Therefore, the energy barrier for contact freezing is smaller than for immersion freezing.

However, the energy barrier alone does not make a nucleation rate, which complicates the comparison between contact and immersion freezing. Since the two approaches are geometrically different, one may happen on each point on a line and the other on any point on a surface. Therefore, if we would be able to formulate nucleation rates out of the two theoretical descriptions, we would get two formulas with different

ACPD
13, 7811–7869, 2013

units on, per unit length and per unit surface. Thus, to decide if in practice, contact freezing is faster than immersion freezing is not straightforward. It may turn out, that contact freezing is slower even if it has the lower energy barrier.

Recently, Gurganus et al. (2011) reported experimental results which contradict the previously mentioned mechanism. Using an improved and modified version of a cold stage (Suzuki et al., 2007) to avoid the point like contact (i.e. the contact between the drop and the IN) and to minimize the temperature variation within the water drop surface, the preferred location to nucleate an ice crystal was investigated. They tested 189 drops and found that there is no preference to form the ice germ at the 3-phase boundary (surface-droplet-air) or 3-phase contact line over the 2-phase contact area.

3 Experimental results and discussion

Contact freezing became an important topic in the 1960s in the context of weather modification. Different instruments were developed, which will be briefly described in the following subsections. Table 1 summarizes previous studies on contact freezing using different instrumentation, IN type, particle and droplet sizes, relative humidities, aerosol particle and droplet concentrations. The first experimental studies focused on the IN properties of different organic materials and AgI; however, nowadays the scientific community is primarily focuses on bioaerosols, mineral dust and volcanic ash particles. Note that most of the studies were conducted with rain drops instead of cloud droplets, not all of them used monodisperse aerosol particles and often the number of collisions is unknown. It is therefore difficult to make a direct comparison between the different studies due to the large variability in the experimental conditions. Below, the most relevant results from each instrument are shown and discussed.

ACPD
13, 7811–7869, 2013

3.1 Cold plate

The cold plate is the oldest reported instrument to study contact freezing (Gokhale and Goold Jr., 1968). The cold plate consists of a metallic surface that is coated with a thin layer of hydrophobic material (e.g. paraffin) to repel water. There are two different ways to perform a contact freezing experiment using this technique. In the most common way, the liquid droplet is placed on the plate and the IN is located at the side of the drop but in touch with it. Thereafter, temperature is decreased until ice formation is observed. It typically uses one drop. Another possibility is to place the drop on the cold plate and then direct an air stream with aerosol particles towards the drop while temperature is reduced until the droplet freezes. In this case it is possible to use more than one drop at the same time. The freezing of the drop(s) can be monitored using a high speed camera or other techniques. The relative humidity and hence evaporation can also be controlled. Figure 5 shows the apparatus used by Shaw et al. (2005) and Durant and Shaw (2005) with its main components.

The use of a single drop with the cold plate results in lower statistics compared to other techniques. However, using single drops and single particles avoids the collision efficiency calculations and allows more precise freezing efficiency calculations. This technique provides useful information regarding the physical processes such as evaporation freezing, volume vs. surface nucleation and particle penetration after the collision takes place.

The first cold plate studies were conducted with polydisperse submicron aerosol particles, whereas the recent studies used large monodisperse aerosol particles such as volcanic ash. Table 2 summarizes the available studies conducted on a cold plate. The average onset freezing temperature (i.e. temperature at which the tested drop freezes) strongly depends on the chemical composition of the IN. Relatively pure AgI and metaldehyde were found to be very good materials to nucleate ice via contact freezing; however their atmospheric relevance is low.

ACPD
13, 7811–7869, 2013

In Gokhale and Goold Jr. (1968) 20 drops were put on the cold plate at the same time and the aerosol particles were dropped on the drops without any mechanical help. The authors claimed that between 500 to 1000 particles reached each drop. A similar strategy was used by Bunker et al. (2012), however they only used one drop instead of 20. Bunker et al. (2012) found that kaolinite nucleates ice by contact freezing at −18 °C, and ATD at −15 °C. The very low calculated FE ($\approx 1.0^{-5}$) suggests that at high temperatures, many collisions are required to nucleate ice. The IN efficiency of the used kaolinite was lower as compared to Pitter and Pruppacher (1973), Svensson et al. (2009) and Ladino et al. (2011b) studies who also used kaolinite. The kaolinite source and the differences in droplet size could explain these discrepancies. It is possible that the used kaolinite samples may have substantial differences in their chemical composition. Note that this limitation is not only related to mineral dust particles and cold stage studies.

Gokhale and Goold Jr. (1968) and Gokhale and Lewinter (1971) showed that the AgI particles remain at the droplet surface after the collision, i.e. there is no particle penetration into the droplet. They also demonstrated that once a collision takes place, the freezing of the droplets needs 16–47 ms to occur. Unfortunately, this behaviour has not been further investigated with other instrumentation. This is very important in order to evaluate the stochastic or deterministic behavior of contact freezing. This is vital information in order to apply relatively simple calculations of ice formation by contact freezing on the basis of determined freezing efficiencies (also termed ice nucleation activity).

Volcanic ash particles from different volcanoes resulted in different freezing temperatures because of differences in chemical composition. The results from Shaw et al. (2005) and Durant and Shaw (2005) reveal very similar freezing temperatures for volcanic ash, glass-rich volcanic ash and soda glass particles. They provide evidence that it does not matter if the contact between the IN and the droplet surface is from the inside or the outside. Durant and Shaw (2005) speculate about evaporation and

ACPD
13, 7811–7869, 2013

its importance in the atmosphere, given that evaporation causes immersed IN to come into contact with the droplet surface which could triggering freezing.

3.2 Wind tunnel

The first wind tunnel was built in 1968 (Pruppacher and Neiburger, 1968; Beard and Pruppacher, 1969) to study collision efficiencies. Vohl (1989) developed an improved version of the UCLA wind tunnel that enabled contact freezing studies. In these studies a supercooled drop is suspended in a vertical air stream. The air mass is prehumidified to avoid evaporation. Particles are injected upstream and eventually hit the levitated supercooled drop. Freezing of the droplets after collisions is detected by a change in its appearance (i.e. opaque). Moreover, the flow balance also changes once the droplet freezes because its terminal velocity changes. Figure 6 shows a schematic of the wind tunnel (Vohl et al., 1999) with its relevant parts.

Figure 7 shows contact freezing results from experiments conducted in a wind tunnel using five different particle types (bacteria, kaolinite, montmorillonite, soot and birch spores) as IN (Pitter and Pruppacher, 1973; Levin and Yankofsky, 1983; Diehl and Mitra, 1998; Diehl et al., 2002). They used almost the same droplet size (220–370 µm in diameter), however, because of the nature of the aerosol particles the IN sizes differed. Soot particles (radii) ranged from 0.05 to 0.1 µm, kaolinite and montmorillonite from 0.05 to 15 µm, birch spores are > 12.5 µm and bacteria are < 0.23 µm (the bacteria cells were passed through a grid of 0.45 µm). Assuming that the particle size influence is small, it is possible to compare these four different data sets as they used similar conditions and were conducted with the same instrument. The authors found that the five tested particles nucleated ice at temperatures higher than necessary for homogeneous freezing. Bacteria initiated ice formation at the highest temperatures (269.7 K). Interestingly, bacteria show a steep increase in the frozen fraction over a very narrow temperature range. The slopes of the frozen fractions with temperature strongly depend on the used IN.

ACPD
13, 7811–7869, 2013

A large uncertainty in the results presented in Fig. 7 is the aerosol particle concentration and hence the number of collisions between particles and droplets since in some of those studies it was neither measured nor controlled. This parameter is important in order to determine the collision rates and freezing efficiencies. Only frozen fractions can be reported which strongly depend on experiment conditions and therefore do not represent true particle properties. The study by Diehl and Mitra (1998) is the only exception where the aerosol concentration was between 10^5–$10^6\,cm^{-3}$, which is several orders of magnitude higher than IN concentrations found within a cloud (Deshler and Vali, 1992; Rogers, 1993; DeMott et al., 2003, 2010). If the collision rates for the used drops, particles and concentrations are given, the freezing efficiencies could be determined.

3.3 Electrodynamic balance (EDB)

The electrodynamic balance is a versatile instrument to study different physical properties and processes with single levitated liquid droplets (e.g. index of refraction, homogeneous ice nucleation, hygroscopicity and evaporation rates). Recently the EDB has been used for contact freezing experiments as well (Svensson et al., 2009). The EDB consists of a double-ring electrode with two end cap electrodes. These concentric rings are supplied with AC and DC voltages. The DC field is used to keep the droplet in a balance (i.e. levitating between the rings) as this field acts against the effect of gravitation. Droplets of different sizes can be generated using an electrically charged syringe-needle system or with a piezoelectric droplet generator. Both systems ensure that the droplets are electrically charged which is a requirement to control them by the electric fields in the EDB. Two CCD (charge coupled device) cameras are used to measure the droplet size via the intensity of light scattered by a laser beam. Fluctuations of the scattered light are used to detect the phase transition from liquid to solid (or solid to liquid) (Duft and Leisner, 2004a,b; Svensson et al., 2009). Figure 8 shows a schematic of the EDB with the alignment of the CCD's and the light source. Charged particles can be injected to collide with the levitating droplet (mainly due to electroscavenging).

ACPD
13, 7811–7869, 2013

The air temperature, relative humidity and the total pressure within the EDB can be measured and adjusted.

So far only one study on contact freezing is published with an EDB (Svensson et al., 2009). In this study, the freezing probability or freezing efficiency of kaolinite particles to nucleate ice crystals is reported. Figure 9 shows that the freezing efficiency increases with decreasing temperature and increasing relative humidity. The RH_w dependence of contact nucleation is hard to understand as the collision efficiency (Sect. 2.1 and Fig. 2) decreases with increasing RH_w due to thermophoresis. However, it could also be interpreted that the freezing efficiency upon collision is secondarily sensitive to RH_w. This dependence requires further investigations.

Since the used kaolinite particles are polydisperse (from 0.3 µm to 2.5 µm in diameter) it could be that the largest particles were responsible for the observed freezing events in Svensson et al. (2009). If this is the case, the phoretic forces are of minor importance. The uncertainties in the reported freezing efficiencies in Svensson et al. (2009) can be reduced if experimental collision efficiencies are determined. Additionally, if monodisperse aerosol particles are used and droplet evaporation is controlled and measured, it will be possible to confirm/reject the dependence of contact nucleation on RH_w.

3.4 Cloud chambers

There are different types of cloud chambers which are able to study the heterogeneous freezing modes independently and/or more than one mode at the same time. In this section the NCAR counter, the Colorado State University (CSU) isothermal cloud chamber, the thermal diffusion chamber and the collision ice nucleation chamber (CLINCH) are described with their corresponding results. Advantages of these flow chambers are continuos flows and known residence times. It is possible to divide those instruments in two different categories, mixing cloud chambers and continuous flow cloud chambers.

ACPD
13, 7811–7869, 2013

3.4.1 Mixing cloud chambers

The NCAR ice nucleus counter is a mixing chamber which was originally built at the National Center for Atmospheric Research (NCAR, Langer et al., 1967); however, new chambers of the same type were built afterwards (e.g. Langer, 1973; Super et al., 2010). The NCAR ice nucleus counter is typically operated as follows. Haze particles, aerosol particles and/or CCN are combined with a humid air mass ($RH_w \approx 80\,\%$) at room temperature. The air stream with the particles is placed at the top of the chamber where its temperature is gradually reduced while the introduced particles are activated as flow descends downward through the chamber (Langer, 1973). Langer et al. (1978) modified the standard NCAR counter to investigate immersion and contact freezing. This modification allows the injection of new particles which can be tested as IN. The particles are introduced in the bottom section of the chamber to interact with the activated cloud droplets at the desired temperature. The chamber wall temperatures are controlled by a cooling system. An acoustic sensor was used to detect ice at the exit of the counter. The currently available NCAR counters do not have the previously mentioned modification.

The NCAR ice nucleus counter studies basically focused on submicron (< 150 nm) AgI particles. In these studies, Brownian motion was the dominant dynamical force responsible for moving the aerosol particles towards the water drops. Langer et al. (1978) determined the freezing probabilities of AgI particles using the mathematical expression from Sax and Goldsmith (1972). They found that the freezing probabilities increased with decreasing temperature from 259 K to 253 K. In addition, an aerosol particle size effect was clearly observed. Particles smaller than 0.02 µm were not active, whereas for particles larger than 0.02 µm the freezing probability increased with increasing particle size.

A static isothermal chamber with much longer residence times than the NCAR counter is the CSU isothermal cloud chamber (ICC). In the ICC the cloud droplets were generated using an ultrasonic nebulizer and then transferred to a stand tube (10 cm in

ACPD
13, 7811–7869, 2013

diameter) to get thermal equilibrium with the filtered cooled air before the cloud is discharged into the chamber (960 L) (Grant and Steele, 1966). Non-hygroscopic aerosol injected into the chamber with dry air and mixed quickly through the chamber volume will collide with drops if no other nucleation mechanism occurs. In the ICC ice formation is monitored in time and particle coagulation is prevented by a dilution procedure (DeMott et al., 1983; DeMott, 1995).

DeMott et al. (1983) observed that contact freezing efficiency was very high for the AgI-type ice nuclei examined at temperatures of 257 K and higher in agreement with Langer et al. (1978). They also found a clear pseudo-first order dependence of ice nucleation by AgI aerosols on droplet concentrations and aerosol size. With the help of the isothermal chamber and the CSU expansion chamber, DeMott (1995) was able to determine that the freezing rates for contact freezing were higher than for the other three heterogeneous freezing modes.

3.4.2 Continuous flow cloud chambers

Another cloud chamber type is the thermal diffusion chamber. These chambers have been widely used to investigate the ice nuclei abilities of aerosol particles in different heterogeneous freezing modes and homogeneous freezing (Schaller and Fukuta, 1979; Hussain and Saunders, 1984; Tomlinson and Fukuta, 1985; Rogers, 1988; Stetzer et al., 2008; Kanji and Abbatt, 2009). All of these devices, some with continuous flow and some not, use temperature gradients between ice coated walls to expose aerosols to ice and water supersaturations. Schaller and Fukuta (1979) built the first thermal diffusion chamber that was able to study contact freezing. The instrument has a wedge-shaped design and consists of two flat plates covered with ice in order to produce saturation with respect to ice. The temperature of both chamber walls can be varied with the top wall being warmer than the bottom wall. It is also possible to have a concentric cylindrical configuration with a vertical orientation of the chamber (Rogers, 1988). For contact freezing, haze particles were formed at subsaturated con-

ACPD
13, 7811–7869, 2013

ditions with respect to water. Once the haze particles were formed the IN were injected into the chamber to allow them to collide with the haze particles.

Schaller and Fukuta (1979) observed a very low rate of nucleation for AgI particles which means that they are not efficient nucleating ice at high temperatures (from 267 K to 265 K). However, these results may be specific to the type of used AgI particles. Metaldehyde was found to be a very good IN at these temperatures forming three orders of magnitude more ice crystals as compared to the used AgI. It could be that the high efficiency was due to the electric-dipolar nature of metaldehyde which increases the number of collisions due to electroscavenging. Unfortunately, metaldehyde was not used in the subsequent contact freezing studies to confirm these observations. Note that collisions were with small haze droplets that are not dilute cloud droplets. Therefore, it is possible that the IN abilities of the tested aerosol particles were influenced by the added liquid solute.

The latest cloud chamber built is CLINCH (Ladino et al., 2011b). It is a continuous flow chamber which consists of two vertical parallel plates with lengths that can be varied between 20 and 80 cm as shown in Fig. 10. CLINCH uses a droplet generator to inject a series of droplets (with a variable frequency) at the top of the chamber. The aerosol particles enter the chamber at the head from both sides with an air flow. Aerosol particles can interact with the liquid droplets at a constant temperature and humidity in the volume between these plates. Both plates have the same temperature which is controlled with a cryostat. An Ice Optical DEtector (IODE) is used to distinguish between liquid droplets and ice crystals by depolarization (Nicolet et al., 2010). CLINCH is able to perform experiments on contact freezing varying the droplet size, particle size, IN type, aerosol particle concentration, residence time and temperature at ice saturation relative humidity.

Ladino et al. (2011b) studied the effect of the IN size and the aerosol particle concentration on the frozen fraction using kaolinite particles and cloud droplets of 12.7 µm in radius. The left panel in Fig. 11 shows that with increasing IN size the onset freezing temperature (defined when 3 % of the droplets freeze) increases. This effect can be

ACPD
13, 7811–7869, 2013

attributed to the increase in the surface area which increases the probability to have more active sites at which the ice germ can form. A similar behavior was previously observed by Langer et al. (1978) and DeMott (1995) using AgI and AgI-AgCl particles. The collision efficiency is similar for both particle sizes (400 and 800 nm) and therefore it does not contribute to the difference between the results for 400 nm and 800 nm particles. There is not a clear difference in the frozen fraction between 400 nm and 800 nm particles for temperatures lower than 248 K for the time spent in the chamber. In CLINCH, the frozen fraction that can be attributed to contact freezing does not exceed 0.4 because of the limited number of collisions during the residence time (5 s) of the droplets in the chamber. Note that this is true for a certain chamber length and droplet size.

The right panel in Fig. 11 shows the frozen fraction for two different aerosol particle concentrations. Keeping the CE constant for a drop-particle size pair, the number of particles within the droplet's sweep-out volume and the number of collected particles by the droplets will increase if the aerosol particle concentration is increased. It results in a larger number of potential IN and active sites interacting with the droplets causing a larger number of nucleated ice crystals. Nevertheless, differences in freezing fractions when using 300 cm^{-3} or 1000 cm^{-3} kaolinite particles were surprisingly small and will be further investigated.

In CLINCH the droplet size is measured accurately at the top section, however its size along the chamber and at the bottom section is uncertain since the droplets shrink due to evaporation. The droplet size is a key parameter when determining the collision efficiency, which in turn is important to determine the freezing efficiency of contact freezing. It is the reason of the high and uncertain freezing efficiencies reported from CLINCH. More research in this direction is needed.

3.5 Freezing efficiency results inter-comparison

In the above sections it was shown that the frozen fraction can be experimentally determined by different instrumentation. In some cases the freezing efficiencies can

ACPD
13, 7811–7869, 2013

also be calculated based on the instrument and available information. However, the reported freezing efficiencies are experiment-dependent. Because kaolinite has been extensively studied with different instrumentation, it was chosen to inter-compare the freezing efficiencies obtained with the wind tunnel, cold plate, EDB and CLINCH. The experiment-dependent kaolinite freezing efficiencies are summarized in Fig. 12.

Although Pitter and Pruppacher (1973) did not calculated/reported the freezing efficiency of their wind tunnel experiments, we used the provided data to calculate their corresponding freezing efficiencies based on some assumptions in order to investigate the role of the aerosol particle concentration on the freezing efficiencies. The three N_{coll} scenarios from the wind tunnel data demonstrate the high variability and sensitivity on calculating the freezing efficiencies. The dependence of freezing efficiency on RH_w reported in Svensson et al. (2009), particle size reported in Bunker et al. (2012) and the two droplet size in Ladino et al. (2011b) is obvious.

Figure 12 also shows theoretical calculations (solid color lines) of $N_{g,contact}$ using Eq. (6) following the procedure described in Hoose et al. (2010). These calculations were conducted for particles with a size of 500 nm, a contact angle of 12.7° and a ΔG of 0.621×10^{-20} J. Note that $N_{g,contact}$ is equivalent to FE. The theoretical calculations show that ice forms at higher temperatures with increasing RH_w. This is in agreement with the observations made by Svensson et al. (2009). Note that the relative humidies for the dry, intermediate and humid conditions of the experiments conducted by Svensson et al. (2009) were not reported. At high RH_w's, the theoretical increase of FE with temperature is very steep and it requires less than 5 K to move from 1.0×10^{-5} to 1.0. This is in contrast to the experimentally obtained/derived FE's. However, at RH_w of 80 % around 10 K are needed to obtain the full FE activation. This temperature trend is closer to the data reported by Pitter and Pruppacher (1973); Svensson et al. (2009) and Ladino et al. (2011b). However, the obvious discrepancies can be attributed to the different experimental conditions and to the assumptions made for the theoretical calculations.

ACPD
13, 7811–7869, 2013

Even though the particle type (kaolinite) is the same in all four studies, the experimental conditions differ substantially. The experimental differences and the high uncertainty in the collision rates are reflected in the calculated kaolinite freezing efficiency. These values differ by several orders of magnitude in the same temperature range, even when similar particle and droplet sizes are used. Although the comparison of the theoretical and experimental results is clearly qualitative, it confirms how sensitive the determination of FE is. That is why better designed experiments or inter-laboratory campaigns (i.e. experiments of contact freezing using different techniques with the same IN samples and similar aerosol particle concentration, comparable RH_w and comparable droplet and particle sizes) are needed to validate the freezing efficiency of contact freezing that could be used in process and climate models.

3.6 Contact freezing versus immersion freezing

A direct qualitative comparison between contact freezing and immersion freezing from experimental results has been done by Pitter and Pruppacher (1973); Levin and Yankofsky (1983); Diehl and Mitra (1998); Diehl et al. (2002); Shaw et al. (2005); Durant and Shaw (2005); Fornea et al. (2009) and Ladino et al. (2011b) using a cold plate, wind tunnel or CLINCH/IMCA. The same particles where either immersed within a droplet (before or during the experiment) or put in contact with the droplet surface (mechanically or due to a flow). Langer et al. (1978), Schaller and Fukuta (1979), DeMott et al. (1983), DeMott (1995) conducted experiments of the other heterogeneous freezing modes in addition to contact freezing in their cloud chambers. However, due to the large complexity in assigning an ice nucleation event to a specific mechanism they are not discussed here.

Figure 13 shows the comparison of contact vs. immersion freeezing experiments conducted in a wind tunnel. Contact freezing occurs at higher temperatures than immersion freezing when bacteria, pollen or kaolinite particles were used. In these experiments, the numbers of ice crystals formed were typically higher than for immersion freezing at a given temperature. Only soot particles show the opposite behavior where

ACPD
13, 7811–7869, 2013

immersion freezing was found to be more efficient than contact freezing. The difference between the two freezing modes for soot is however, much smaller than for kaolinite particles. Kaolinite particles show a difference in the onset freezing temperature of around 10 K whereas the other tested particles only show a difference of less than 4 K.

Table 2 summarizes the comparison between immersion and contact freezing from the experiments conducted with a cold plate. Two volcanic ash particles and two organic particles that behave like glasses were investigated. The differences in the onset freezing temperature vary between 3 K and 7 K. The differences are consistent even if different cold plates and IN are used. All cold plate experiments were conducted using different particle and droplet sizes which complicate the comparison of results from different authors. These experiments did not report the frozen fraction as they used a single droplet and a single aerosol particle.

Another comparison between these two modes was done by Ladino et al. (2011b). The contact freezing experiments were conducted in CLINCH whereas the immersion freezing experiments used the immersion freezing chamber IMCA (Lüönd et al., 2010). This comparison is limited by having used different chambers and different droplet sizes, but uses the same kaolinite particles of the same size, particle generator, size selection technique and detector. Figure 14 shows the results using two different particle sizes. As mentioned in Sect. 3.4, the number of ice crystals in CLINCH is limited by the number of collisions to a frozen fraction of 0.4. For both particles sizes 400 nm (left) and 800 nm (right) there is a clear difference in the onset freezing temperature and in the frozen fraction being more pronounced for the 400 nm particles. This means that CLINCH/IMCA also shows that contact freezing is initiated at higher temperature than immersion freezing. This comparison has a similar limitation as the one from the wind tunnel studies because the number of particles that collides with the droplet on average is below one hence it is smaller than the single particle immersed within each droplet in the IMCA experiments. Furthermore the influence of the droplet size in CLINCH is not clear since it is shrinking which changes its collision efficiency. This will be investigated further in the future.

ACPD
13, 7811–7869, 2013

The comparison between these two modes is more precise in the cold plate experiments as it uses one IN per drop in both contact and immersion freezing. However, this comparison can be improved if the IN surface area which enters in contact with the droplet (or the line length of the three-phase boundary according to the three-phase-model in Sect. 2.3.4) is estimated and used instead of the number of particles. The aerosol particle surface area for immersion freezing experiments is constant over time, however, this surface area in the contact freezing experiments in the wind tunnel, EDB and CLINCH studies increases with time with the exception of cold plate studies where only one aerosol particle per drop was used. For the wind tunnel experiments it is unknown if the IN/drop ratio in contact and immersion freezing mode is comparable. The comparison with CLINCH is also not adequate as their contact freezing experiments are not normalized to the number of collisions, whereas in IMCA the particle-droplet ratio is always one. However, if the shrinking droplet size from CLINCH is estimated accurately, a better calculation of N_{coll} can be obtained and hence a normalization will be possible in contrast with the data shown in Fig. 12. Thus simultaneous comparable measurements of contact and immersion freezing are urgently needed.

As shown above, immersion freezing and contact freezing data are often compared to each other. However, a fair comparison between both modes is rather difficult because a number of parameters should be controlled or constrained. We suggest here a possible approach for a fair comparison (see Fig. 15).

The freezing efficiencies or the frozen fractions for both modes can only be directly compared, when droplets of one size are exposed to the same number of particles of the same size for the same time. The implications not only for experiments on both modes but also for natural clouds with conditions where contact freezing is possible is as follows. Under pure immersion freezing conditions (all particles are immersed in a droplet and each droplet contains only one particle) the droplet freezes after some time since the IN surface area in contact with the supercooled liquid is constant over time. In this setting immersion freezing scales linearly with time and surface area of the

ACPD
13, 7811–7869, 2013

IN:

$$\ln\left(\frac{N_{\text{frozen}}(t)}{N_{\text{total}}}\right) = J_{\text{imm}}(T)\cdot S(t)\cdot t, \tag{9}$$

where J_{imm} is the nucleation rate due to immersion freezing as a function of temperature (T), and $S(t)$ the total area of immersed particles as a function of time (t).

Under pure contact freezing conditions, once an IN collides with a supercooled droplet it can cause freezing of the droplet due to contact freezing. If this does not happen, assume that the IN gets immersed into the droplet and can then act as an immersion freezing nucleus. If immersion freezing does not cause the droplet to freeze under the prevailing conditions, another IN can collide with the droplet. Again, contact freezing can take place or immersion freezing after the particle gets immersed into the droplet. This cycle continues until the droplet freezes by one of the two processes. Here, contact freezing is constant over time (as is the collision rate) while the number (and thus the surface area) of immersed particles in a droplet increases linearly with time causing the immersion freezing process to be a function of time squared. To unambiguously determine, which freezing process caused the droplets to freeze requires studying the time-dependence of the freezing rocess:

$$\ln\left(\frac{N_{\text{frozen}}(t)}{N_{\text{total}}}\right) = \left[J_{\text{imm}}(T)\cdot S(t)\cdot t\right] + \left[\text{FE}(T)\cdot n_{\text{c}}\cdot t\right], \tag{10}$$

$$= \left[J_{\text{imm}}(T)\cdot S_{\text{p}}\cdot n_{\text{c}}\cdot t^2\right] + \left[\text{FE}(T)\cdot n_{\text{c}}\cdot t\right], \tag{11}$$

where S_{p} is the aerosol particle surface area, and n_{c} the collision rate (N_{coll}/t).

3.7 Parameterizations

In order to consider contact freezing in numerical models, several parameterizations were derived for the IN concentrations (Young, 1974b; Meyers et al., 1992; Phillips

ACPD
13, 7811–7869, 2013

et al., 2008; Morrison et al., 2008; Hoose et al., 2010). Because the wind tunnel and the CLINCH experiments yield a frozen fraction but not the number of IN, we compare the experimental wind tunnel and CLINCH data with the parameterized frozen fractions from Diehl et al. (2006) in Fig. 16. Good agreement between the wind tunnel data and mineral dust, bacteria and pollen can be seen because these data were used to obtain the parameterization. However, soot in the wind tunnel initiated freezing at much colder temperatures than the parameterization suggests. This is because the soot parameterization is based on the data by Gorbunov et al. (2001). It is however questionable if the freezing of soot in the Gorbunov et al. (2001) study is really due to contact nucleation or rather due to deposition nucleation. The much colder freezing temperatures of the soot measured by Diehl and Mitra (1998) are thought to be caused by an organic coating of the particles emitted as a by product of the used kerosene burner (K. Diehl, personal communication, 2012). The kerosene soot burner data show a freezing onset and increase of frozen fraction with decreasing temperature that is comparable to what is found for two different sizes of kaolinite using CLINCH. Kaolinite in CLINCH freezes at much colder temperatures than in the wind tunnel. This range in freezing onset and increase of frozen fraction with decreasing temperature shows the uncertainty in the data and will translate in an equally large uncertainty in the parameterization of the frozen fraction.

4 Conclusions

There is experimental evidence for contact freezing to act as proposed by Cooper (1974), Durant and Shaw (2005) and Djikaev and Ruckenstein (2008), however it is unclear yet, why contact freezing is the most efficient ice nucleation mode. More and better controlled experiments are needed to validate the proposed hypotheses by Cooper (1974) and Durant and Shaw (2005) which so far are the most promising ideas. Cooper's hypothesis could be tested if both the particle and the droplet could be ob-

ACPD
13, 7811–7869, 2013

served in a high temporal resolution instrument and with a precise control of the relative humidity.

Laboratory experiments designed to specifically quantify contact freezing indicate that contact freezing initiates ice formation at the highest temperatures. A difference of around 1–10 K in the onset freezing temperatures and in the number of formed ice crystals at a given temperature between contact and immersion freezing was found when using the wind tunnel with different IN. Similarly, a difference of 5–8 K in the onset freezing temperatures and in the number of formed ice crystals was observed for two different particle sizes when kaolinite particles in the CLINCH/IMCA flow chambers were compared. A difference of around 3–7 K was found in the onset freezing temperatures when using the cold plate with different volcanic ash particles. Experiments conducted in the mixing chamber also showed a clear difference between contact freezing, condensation/immersion freezing, and deposition nucleation. Therefore, contact freezing is clearly distinguished from the other heterogeneous freezing modes and it is the most efficient pathway to nucleate ice crystals.

The atmospheric IN concentration is much smaller than the values used in the laboratory experiments. Therefore, the atmospheric relevance of contact freezing is unclear. A quantitative calculation of the frozen fraction is needed to determine the maximum freezing efficiencies. Disagreements with theoretical collection rates remain and need to be investigated in future. Most of the experimental studies did not report the collision rates and therefore give only experiment-specific frozen fractions but no experiment-independent freezing efficiencies. Once collision rates are known, the uncertainty in the freezing efficiency calculation will be substantially reduced. It will allow an intercomparison between data sets from different experiments and an extrapolation of the laboratory results to atmospheric conditions is possible. Especially, more experiments with cloud droplets and monodisperse submicron aerosol particles taking into account the aerosol particle concentration and RH_w are needed.

Cold plate studies suggest that the difference in the temperature at which an ice germ forms in the contact and immersion freezing mode could be caused by the interaction

ACPD
13, 7811–7869, 2013

between the different phases but does not involve a collision energy. However, wind tunnel and flow chamber experiments where collisions take place also show a difference between these two heterogeneous freezing modes. It is difficult to conclude if the ice germs form at higher temperatures during contact freezing than immersion freezing due to the collision (IN-droplet) or due to the phase interactions or if it is a combination of both factors. There are some indications for both theories but they are not proven as the experimental data have some limitations. In cold plate experiments large particles were used, thus the surface area of the particles which comes in contact with the droplets is much larger than the submicron particles which were used in wind tunnel studies and in CLINCH. In cases where collisions are present, the surface area that comes in contact with the droplet is not known. This surface may be larger in the wind tunnel and flow chambers than in the cold plate experiments because of the collision kinetic energy.

In a real cloud, more than one freezing mechanism can take place at the same time. It will be interesting to perform experiments where a single IN is immersed in a liquid droplet and thereafter more IN are injected that collide with the droplet/IN system to simulate the real competition between immersion and contact freezing within a mixed-phase cloud. This type of experiment will tell us if contact freezing matters in this scenario. Mixing chambers like the NCAR ice nucleus counter or the CSU-CIC can be perfectly adjusted to do that.

New instrumentation is needed where the atmospheric conditions can be reproduced as closely as possible in order to increase the usefulness of the produced data. New instrumentation should measure and control the important parameters for contact freezing (RH_w, a, r, N_a). Additionally, field measurements on contact freezing are urgently needed since these studies are very scarce (e.g. Davis and Auer, 1972). One limitation to perform field measurements is to overcome the slow collection rates. The collection rates could be enhanced if the aerosol concentration and the residence time are increased. The aerosol concentration can be increase with the help of an aerosol particle concentrator and/or a counter flow virtual impactor (it is commonly used to separate

ACPD
13, 7811–7869, 2013

cloud droplets or ice crystals from interstitial aerosols but it is also possible to use it as an aerosol concentrator, Slowik et al., 2011). Field measurements will allow us to validate the laboratory experiments and their data will be very valuable for validation of numerical models (cloud resolving, regional and global climate models).

Almost all previous comparisons between immersion freezing and contact freezing were done with the aim to study the IN ability in both modes and to infer which mode is more efficient. However, an accurate direct comparison is not possible (or has not yet been done) because even when using the same IN and the same particle size the experimental conditions are different. The number of particles within or in contact with the droplet in both modes is different. Assuming that the ratio particle/droplet is the same, the comparison is still not completely fair because in the immersion mode the whole IN surface is immersed, therefore the whole IN plays a role in that case. In contrast, in contact freezing only a part of the IN surface is in contact with the droplet, therefore only a small part of the IN is responsible for freezing. In order to directly compare and validate the available instrumentation, it would be interesting to perform a contact nucleation intercomparison where all experiments use the same chemical composition and particle size at a defined temperature range.

Acknowledgements. The authors would like to thank Zamin Kanji, Felix Lüönd, Cedric Chou, Andre Welti, and Vivek Sant for their valuable contribution during the interesting discussions. We also thank Corinna Hoose for the $N_{g,contact}$ calculations and Alexei Kiselev for sharing his ideas, which are indicated in Fig. 15 and the corresponding formulas. This work was supported by the Swiss National Foundation (SNF) with the following projects: 200021-107663/1 and 200021-127275.

References

Abbatt, J., Benz, S., Cziczo, D., Kanji, Z., Lohmann, U., and Möhler, O.: Solid ammonium sulfate aerosols as ice nuclei: a pathway for cirrus cloud formation, Science, 313, 1770–1773, 2006. 7813

ACPD
13, 7811–7869, 2013

Andronache, C., Grönholm, T., Laakso, L., Phillips, V., and Venäläginen, A.: Scavenging of ultrafine particles by rainfall at a boreal site: observations and model estimations, Atmos. Chem. Phys., 6, 4739–4754, doi:10.5194/acp-6-4739-2006, 2006. 7818, 7819

Beard, K.: Experimental and numerical collision efficiency for submicron particles scavenged by small rain drops, J. Atmos. Sci., 31, 1595–1603, 1974. 7814, 7818

Beard, K. and Pruppacher, H.: A determination of the terminal velocity and drag of small water drops by means of a wind tunnel, J. Atmos. Sci., 26, 1066–1072, 1969. 7827

Bunker, K. W., China, S., Mazzoleni, C., Kostinski, A., and Cantrell, W.: Measurements of ice nucleation by mineral dusts in the contact mode, Atmos. Chem. Phys. Discuss., 12, 20291–20309, doi:10.5194/acpd-12-20291-2012, 2012. 7826, 7834, 7852, 7865

Chen, J.-P., Hazra, A., and Levin, Z.: Parameterizing ice nucleation rates using contact angle and activation energy derived from laboratory data, Atmos. Chem. Phys., 8, 7431–7449, doi:10.5194/acp-8-7431-2008, 2008. 7821

Cooper, W.: A possible mechanism for contact nucleation, J. Atmos. Sci., 31, 1832–1837, 1974. 7814, 7821, 7822, 7839, 7856

Croft, B., Lohmann, U., Martin, R. V., Stier, P., Wurzler, S., Feichter, J., Posselt, R., and Ferrachat, S.: Aerosol size-dependent below-cloud scavenging by rain and snow in the ECHAM5-HAM, Atmos. Chem. Phys., 9, 4653–4675, doi:10.5194/acp-9-4653-2009, 2009. 7818

Davis, C. and Auer, A.: The possibility of collision nucleation by an AgI aerosol in an orographic cap cloud, J. Rech. Atmos., 12, 287–307, 1972. 7841

DeMott, P.: An exploratory study of ice nucleation by soot aerosols, J. Appl. Meteorol., 29, 1072–1079, 1990. 7813

DeMott, P.: Quantitative descriptions of ice formation mechanisms of silver iodide-type aerosols, Atmos. Res., 38, 63–99, 1995. 7814, 7815, 7822, 7831, 7833, 7835, 7852

DeMott, P., Finnegan, W., and Grant, L.: An application of chemical kinetic theory and methodology to characterize the ice nucleating properties of aerosols used for weather modification, J. Appl. Meteorol., 22, 1190–1203, 1983. 7814, 7815, 7831, 7835, 7852

DeMott, P., Sassen, K., Poellot, M., Baumgardner, D., Rogers, D., Brooks, S., Prenni, A., and Kreidenweis, S.: African dust aerosols as atmospheric ice nuclei, Geophys. Res. Lett., 30, 1732, 14655–14660, 2003. 7828

ACPD
13, 7811–7869, 2013

DeMott, P., Prenni, A., Liu, X., Kreidenweis, S., Petters, M., Twohy, C., Richardson, M., Eidhammer, T., and Rogers, D.: Predicting global atmospheric ice nuclei distributions and their impacts on climate, P. Natl. Acad. Sci. USA, 107, 11217, 11217–11222, 2010. 7828

Deshler, T.: Measurements of the rate at which submicron aerosol particles are scavenged by water drops, J. Aerosol Sci., 16, 399–406, 1985. 7818

Deshler, T. and Vali, G.: Atmospheric concentrations of submicron contact-freezing nuclei, J. Atmos. Sci., 49, 773–784, 1992. 7815, 7828, 7852

Diehl, K. and Mitra, S.: A laboratory study of the effects of a kerosene-burner exhaust on ice nucleation and the evaporation rate of ice crystals, Atmos. Environ., 32, 3145–3151, 1998. 7813, 7814, 7815, 7822, 7827, 7828, 7835, 7839, 7852, 7860, 7866, 7869

Diehl, K., Quick, C., Matthias-Maser, S., Mitra, S., and Jaenicke, R.: The ice nucleating ability of pollen, Part 1: Laboratory studies in deposition and condensation freezing modes, Atmos. Res., 58, 75–87, 2001. 7822

Diehl, K., Matthias-Maser, S., Jaenicke, R., and Mitra, S.: The ice nucleating ability of pollen, Part 2: Laboratory studies in immersion and contact freezing modes, Atmos. Res., 61, 125–133, 2002. 7814, 7827, 7835, 7852, 7860, 7866, 7869

Diehl, K., Simmel, M., and Wurzler, S.: Numerical sensitivity studies on the impact of aerosol properties and drop freezing modes on the glaciation, microphysics and dynamics of clouds, J. Geophys. Res., 111, D07202, doi:10.1029/2005JD005884, 2006. 7839, 7869

Djikaev, Y. and Ruckenstein, E.: Thermodynamics of heterogeneous crystal nucleation in contact and immersion modes, J. Phys. Chem. A, 112, 11677–11687, 2008. 7820, 7823, 7839, 7857

Djikaev, Y., Tabazadeh, A., Hamill, P., and Reiss, H.: Thermodynamic conditions for the surface-stimulated crystallization of atmospheric droplets, J. Phys. Chem. A, 106, 10247–10253, 2002. 7820

Duft, D. and Leisner, T.: Laboratory evidence for volume-dominated nucleation of ice in supercooled water microdroplets, Atmos. Chem. Phys., 4, 1997–2000, doi:10.5194/acp-4-1997-2004, 2004a. 7828, 7861

Duft, D. and Leisner, T.: The index of refraction of supercooled solutions determined by the analysis of optical rainbow scattering from levitated droplets, Int. J. Mass Spectrom., 233, 61–65, 2004b. 7828

ACPD
13, 7811–7869, 2013

Durant, A. and Shaw, R.: Evaporation freezing by contact nucleation inside-out, Geophys. Res. Lett., 32, L20814, doi:10.1029/2005GL024175, 2005. 7814, 7815, 7825, 7826, 7835, 7839, 7852, 7853

Dymarska, M., Murray, B., Sun, L., Eastwood, M., Knopf, D., and Bertram, A.: Deposition ice nucleation on soot at temperatures relevant for the lower troposphere, J. Geophys. Res., 111, D04204, doi:10.1029/2005JD006627, 2006. 7813

Fletcher, A.: High-temperature contact nucleation of supercooled water by organic chemicals, J. Appl. Meteorol., 11, 988–993, 1972. 7852

Fletcher, N.: Active sites and ice crystal nucleation, J. Atmos. Sci., 26, 1266–1278, 1969. 7814, 7820

Fletcher, N.: Notes and correspondence: on contact nucleation, J. Atmos. Sci., 27, 1098–1099, 1970. 7814, 7820

Fornea, A., Brooks, S., Dooley, J., and Saha, A.: Heterogeneous freezing of ice on atmospheric aerosols containing ash, soot, and soil, J. Geophys. Res., 114, D13201, doi:10.1029/2009JD011958, 2009. 7815, 7835, 7852, 7853

Friedman, B., Kulkarni, G., Beránek, J., Zelenyuk, A., Thornton, J., and Cziczo, D.: Ice nucleation and droplet formation by bare and coated soot particles, J. Geophys. Res., 116, D17203, doi:10.1029/2011JD015999, 2011. 7813

Fukuta, N.: A study of a mechanism for contact ice nucleation, J. Atmos. Sci., 32, 1597–1603, 1975. 7814, 7822, 7852, 7853

Gokhale, N. and Goold Jr., J.: Droplet freezing by surface nucleation, J. Appl. Meteorol., 7, 870–874, 1968. 7816, 7825, 7826, 7852, 7853

Gokhale, N. and Lewinter, O.: Microcinematographic studies of contact nucleation, J. Appl. Meteorol., 10, 469–473, 1971. 7826, 7852, 7853

Gokhale, N. and Spengler, J.: Freezing of freely suspended, supercooled water drops by contact nucleation, J. Appl. Meteorol., 11, 157–160, 1972. 7852

Gorbunov, B., Baklanov, A., Kakutkina, N., Windsor, H., and Toumi, R.: Ice nucleation on soot particles, J. Atmos. Sci., 32, 199–215, 2001. 7813, 7839

Grant, L. and Steele, R.: The calibration of silver iodide generators, B. Am. Meteorol. Soc., 47, 713–717, 1966. 7831

Greenfield, S.: Rain scavenging of radioactive particulate matter from the atmosphere, J. Atmos. Sci., 14, 115–125, 1957. 7814, 7818

ACPD
13, 7811–7869, 2013

Guenadiev, N.: Sur le mécanisme de congélation des gouttes d'eau sous l'influence d'un aerosol d'iodure d'argent, J. Rech. Atmos, 4, 81–91, 1970. 7820
Gurganus, C., Kostinski, A., and Shaw, R.: Fast imaging of freezing drops: no preference for nucleation at the contact line, J. Phys. Chem. Lett., 2, 1449–1454, 2011. 7824
Herbert, F. and Beheng, K.: Scavenging of airborne particles by collision with water drops – model studies on the combined effect of essential microdynamic mechanisms, Meteorol. Atmos. Phys., 35, 201–211, 1986. 7818
Hoose, C. and Möhler, O.: Heterogeneous ice nucleation on atmospheric aerosols: a review of results from laboratory experiments, Atmos. Chem. Phys., 12, 9817–9854, doi:10.5194/acp-12-9817-2012, 2012. 7813, 7815
Hoose, C., Kristjánsson, J., Chen, J., and Hazra, A.: A classical-theory-based parameterization of heterogeneous ice nucleation by mineral dust, soot, and biological particles in a global climate model, J. Atmos. Sci., 67, 2483–2503, 2010. 7815, 7821, 7822, 7834, 7839
Hussain, K. and Saunders, C.: Ice nucleus measurement with a continuous flow chamber, Q. J. Roy. Meteorol. Soc., 110, 75–84, 1984. 7831
Isaac, G. and Douglas, R.: Another "time lag" in the activation of atmospheric ice nuclei, J. Appl. Meteorol., 11, 490–493, 1972. 7818
Kanji, Z. and Abbatt, J.: The University of Toronto Continuous Flow Diffusion Chamber (UT-CFDC): a simple design for ice nucleation studies, Aerosol Sci. Technol., 43, 730–738, 2009. 7831
Ladino, L.: Experimental study on collection efficiency and contact freezing of aerosols in a new collision chamber, Ph D. Thesis, ETH Zurich, Zurich, Switzerland, 2011. 7854, 7863
Ladino, L., Stetzer, O., Hattendorf, B., Günther, D., Croft, B., and Lohmann, U.: Experimental study of collection efficiencies between submicron aerosols and cloud droplets, J. Atmos. Sci., 68, 1853–1864, 2011a. 7818
Ladino, L., Stetzer, O., Lüönd, F., Welti, A., and Lohmann, U.: Contact freezing experiments of kaolinite particles with cloud droplets, J. Geophys. Res, 116, D22202, doi:10.1029/2011JD015727, 2011b. 7814, 7815, 7826, 7832, 7834, 7835, 7836, 7852, 7865, 7869
Lai, K., Dayan, N., and Kerker, M.: Scavenging of aerosol particles by a falling water drop, J. Atmos. Sci., 35, 674–682, 1978. 7818
Langer, G.: Evaluation of NCAR ice nucleus counter, Part 1: Basic operation, J. Appl. Meteorol., 12, 1000–1011, 1973. 7830

ACPD
13, 7811–7869, 2013

Langer, G., Rosinski, J., and Edwards, P.: A continuous ice nucleus counter and its applications to tracking in the troposphere, J. Appl. Meteorol., 6, 114–125, 1967. 7830
Langer, G., Cooper, G., Nagamoto, C., and Rosinski, J.: Ice nucleation mechanisms of submicron monodispersed silver iodide, 1, 5-dihydroxynaphthalene and phloroglucinol aerosol particles, J. Appl. Meteorol., 17, 1039–1048, 1978. 7814, 7815, 7830, 7831, 7833, 7835, 7852
Lau, K. and Wu, H.: Warm rain processes over tropical oceans and climate implications, Geophys. Res. Lett., 30, 2290, doi:10.1029/2003GL018567, 2003. 7812
Leong, K., Beard, K., and Ochs III, H.: Laboratory measurements of particle capture by evaporating cloud drops, J. Atmos. Sci., 39, 1130–1140, 1982. 7818
Levin, Z. and Yankofsky, S.: Contact versus immersion freezing of freely suspended droplets by bacterial ice nuclei, J. Climate, 22, 1964–1966, 1983. 7814, 7815, 7827, 7835, 7852, 7860, 7866, 7869
Lohmann, U.: Possible aerosol effects on ice clouds via contact nucleation, J. Atmos. Sci., 59, 647–656, 2002. 7815
Lohmann, U. and Diehl, K.: Sensitivity studies of the importance of dust ice nuclei for the indirect aerosol effect on stratiform mixed-phase clouds, J. Atmos. Sci., 63, 968–982, 2006. 7812
Lohmann, U. and Feichter, J.: Global indirect aerosol effects: a review, Atmos. Chem. Phys., 5, 715–737, doi:10.5194/acp-5-715-2005, 2005. 7812
Lüönd, F., Stetzer, O., Welti, A., and Lohmann, U.: Experimental study on the ice nucleation ability of size-selected kaolinite particles in the immersion mode, J. Geophys. Res., 115, D14201, doi:10.1029/2009JD012959, 2010. 7814, 7836
Marcolli, C., Gedamke, S., Peter, T., and Zobrist, B.: Efficiency of immersion mode ice nucleation on surrogates of mineral dust, Atmos. Chem. Phys., 7, 5081–5091, doi:10.5194/acp-7-5081-2007, 2007. 7814
Meyers, M., Demott, P., and Cotton, W.: New primary ice-nucleation parameterizations in an explicit cloud model, J. Appl. Meteorol., 31, 708–721, 1992. 7815, 7816, 7838
Möhler, O., Büttner, S., Linke, C., Schnaiter, M., Saathoff, H., Stetzer, O., Wagner, R., Krämer, M., Mangold, A., Ebert, V., and Schurath, U.: Effect of sulfuric acid coating on heterogeneous ice nucleation by soot aerosol particles, J. Geophys. Res., 110, D11210, doi:10.1029/2004JD005169, 2005. 7813

ACPD
13, 7811–7869, 2013

Morrison, H., Pinto, J., Curry, J., and McFarquhar, G.: Sensitivity of modeled arctic mixed-phase stratocumulus to cloud condensation and ice nuclei over regionally varying surface conditions, J. Geophys. Res., 113, D05203, doi:10.1029/2007JD008729, 2008. 7839

Mossop, S.: Atmospheric ice nuclei, Z. Angew. Math. Phys., 14, 456–486, 1963. 7815

Murray, B., Wilson, T., Dobbie, S., Cui, Z., Al-Jumur, S., Möhler, O., Schnaiter, M., Wagner, R., Benz, S., Niemand, M., Saathoff, H., Ebert, V., Wagner, S., and Kärcher, B.: Heterogeneous nucleation of ice particles on glassy aerosols under cirrus conditions, Nat. Geosci., 3, 233–237, 2010. 7813

Murray, B., O'Sullivan, D., Atkinson, J., and Webb, M.: Ice nucleation by particles immersed in supercooled cloud droplets, Chem. Soc. Rev., 41, 6519–6554, doi:10.1039/c2cs35200a, 2012. 7815

Nicolet, M., Stetzer, O., Lüönd, F., Möhler, O., and Lohmann, U.: Single ice crystal measurements during nucleation experiments with the depolarization detector IODE, Atmos. Chem. Phys., 10, 313–325, doi:10.5194/acp-10-313-2010, 2010. 7832

Niedermeier, D., Hartmann, S., Shaw, R. A., Covert, D., Mentel, T. F., Schneider, J., Poulain, L., Reitz, P., Spindler, C., Clauss, T., Kiselev, A., Hallbauer, E., Wex, H., Mildenberger, K., and Stratmann, F.: Heterogeneous freezing of droplets with immersed mineral dust particles – measurements and parameterization, Atmos. Chem. Phys., 10, 3601–3614, doi:10.5194/acp-10-3601-2010, 2010. 7814

Park, S., Jung, C., Jung, K., Lee, B., and Lee, K.: Wet scrubbing of polydisperse aerosols by freely falling droplets, J. Aerosol Sci., 36, 1444–1458, 2005. 7818, 7819

Phillips, V., DeMott, P., and Andronache, C.: An empirical parameterization of heterogeneous ice nucleation for multiple chemical species of aerosol, J. Atmos. Sci., 65, 2757–2783, 2008. 7838

Pitter, R. and Pruppacher, H.: A wind tunnel investigation of freezing of small water drops falling at terminal velocity in air, Q. J. Roy. Meteorol. Soc., 99, 540–550, 1973. 7814, 7815, 7822, 7826, 7827, 7834, 7835, 7852, 7860, 7865, 7866, 7869

Pranesha, T. and Kamra, A.: Scavenging of aerosol particles by large water drops, 1. Neutral case, J. Geophys. Res., 101, 373–380, 1996. 7818

Pruppacher, H. and Klett, J.: Microphysics of Clouds and Precipitation, Reidel, Dordrecht, 954 pp., 1997. 7813, 7815, 7820, 7822

ACPD
13, 7811–7869, 2013

Pruppacher, H. R. and Neiburger, M.: Design and performance of the UCLA cloud tunnel. Proceedings of the International Conference on Cloud Physics, Toronto, Canada, 389–392, 1968. 7827
Rau, W.: Über die Wirkungsweise der Gerfrierkerne im unterkühlten Wasser, Z. Naturforsch., 5, 667–675, 1950. 7814
Rogers, D.: Development of a continuous flow thermal gradient diffusion chamber for ice nucleation studies, Atmos. Res., 22, 149–181, 1988. 7831
Rogers, D.: Measurements of natural ice nuclei with a continuous flow diffusion chamber, Atmos. Res., 29, 209–228, 1993. 7828
Rosinski, J. and Nagamoto, C.: Contact nucleation of ice by natural aerosol particles, J. Aerosol Sci., 7, 1–4, 1976. 7814, 7852, 7853
Sax, R. and Goldsmith, P.: Nucleation of water drops by Brownian contact with AgI and other aerosols, Q. J. Roy. Meteorol. Soc., 98, 60–72, 1972. 7830, 7852
Schaller, R. and Fukuta, N.: Ice nucleation by aerosol particles: experimental studies using a wedge-shaped ice thermal diffusion chamber, J. Atmos. Sci., 36, 1788–1802, 1979. 7814, 7831, 7832, 7835, 7852
Shaw, R., Durant, A., and Mi, Y.: Heterogeneous surface crystallization observed in undercooled water, J. Phys. Chem. B, 109, 9865–9868, 2005. 7814, 7815, 7825, 7826, 7835, 7852, 7853, 7858
Slinn, W. and Hales, J.: A reevaluation of the role of thermophoresis as a mechanism of in-and below-cloud scavenging, J. Atmos. Sci., 28, 1465–1471, 1971. 7814, 7818
Slowik, J. G., Cziczo, D. J., and Abbatt, J. P. D.: Analysis of cloud condensation nuclei composition and growth kinetics using a pumped counterflow virtual impactor and aerosol mass spectrometer, Atmos. Meas. Tech., 4, 1677–1688, doi:10.5194/amt-4-1677-2011, 2011. 7842
Stetzer, O., Baschek, B., Lüönd, F., and Lohmann, U.: The Zurich Ice Nucleation Chamber (ZINC) – a new instrument to investigate atmospheric ice formation, Aerosol Sci. Technol., 42, 64–74, 2008. 7831
Stubenrauch, C. J., Cros, S., Guignard, A., and Lamquin, N.: A 6-year global cloud climatology from the Atmospheric InfraRed Sounder AIRS and a statistical analysis in synergy with CALIPSO and CloudSat, Atmos. Chem. Phys., 10, 7197–7214, doi:10.5194/acp-10-7197-2010, 2010. 7812

ACPD
13, 7811–7869, 2013

Super, A., Boe, B., Heimbach Jr., J., McPartland, J., and Langer, G.: Comparison of silver iodide outputs from two different generators and solutions measured by acustic ice nucleus counters, J. Weather Mod., 42, 49–60, 2010. 7830

Suzuki, S., Nakajima, A., Yoshida, N., Sakai, M., Hashimoto, A., Kameshima, Y., and Okada, K.: Freezing of water droplets on silicon surfaces coated with various silanes, Chem. Phys. Lett., 445, 37–41, 2007. 7824

Svensson, E. A., Delval, C., von Hessberg, P., Johnson, M. S., and Pettersson, J. B. C.: Freezing of water droplets colliding with kaolinite particles, Atmos. Chem. Phys., 9, 4295–4300, doi:10.5194/acp-9-4295-2009, 2009. 7814, 7815, 7826, 7828, 7829, 7834, 7852, 7862, 7865

Tabazadeh, A., Djikaev, Y., and Reiss, H.: Surface crystallization of supercooled water in clouds, P. Natl. Acad. Sci. USA, 99, 15873–15878, 2002. 7820

Tinsley, B., Rohrbaugh, R., and Hei, M.: Electroscavenging in clouds with broad droplet size distributions and weak electrification, Atmos. Res., 59, 115–135, 2001. 7818

Tomlinson, E. and Fukuta, N.: A new horizontal gradient, continuous flow, ice thermal diffusion chamber, J. Atmos. Ocean. Technol., 2, 448–467, 1985. 7831

Trenberth, K., Fasullo, J., and Kiehl, J.: Earth's global energy budget, B. Am. Meteorol. Soc., 90, 311–323, 2009. 7812

Vali, G.: Nucleation terminology, B. Am. Meteorol. Soc., 66, 1426–1427, 1985. 7814, 7815, 7816

Vali, G.: Ice Nucleation-Theory: a Tutorial, in: NCAR/ASP 1999 Summer Colloquium, 14–25 June 1999, Boulder, Colorado, USA, 1999. 7813

Vali, G.: Repeatability and randomness in heterogeneous freezing nucleation, Atmos. Chem. Phys., 8, 5017–5031, doi:10.5194/acp-8-5017-2008, 2008. 7814

Vohl, O.: Die dynamischen Charakteristika des Mainzer vertikalen Windkanals. Diplom. thesis, Institut für Physik der Atmosphäre, Universität Mainz. Germany, 1989. 7827

Vohl, O., Mitra, S., Wurzler, S., and Pruppacher, H.: A wind tunnel study of the effects of turbulence on the growth of cloud drops by collision and coalescence, J. Atmos. Sci., 56, 4088–4099, 1999. 7827, 7859

Vohl, O., Mitra, S., Diehl, K., Huber, G., Wurzler, S., Kratz, K., and Pruppacher, H.: A wind tunnel study of turbulence effects on the scavenging of aerosol particles by water drops, J. Atmos. Sci., 58, 3064–3072, 2001. 7818

ACPD
13, 7811–7869, 2013

Von Blohn, N., Mitra, S., Diehl, K., and Borrmann, S.: The ice nucleating ability of pollen, Part 3: New laboratory studies in immersion and contact freezing modes including more pollen types, Atmos. Res., 78, 182–189, 2005. 7814, 7815, 7852

Wagner, R., Möhler, O., Saathoff, H., Schnaiter, M., Skrotzki, J., Leisner, T., Wilson, T. W., Malkin, T. L., and Murray, B. J.: Ice cloud processing of ultra-viscous/glassy aerosol particles leads to enhanced ice nucleation ability, Atmos. Chem. Phys., 12, 8589–8610, doi:10.5194/acp-12-8589-2012, 2012. 7813

Wang, B., Lambe, A., Massoli, P., Onasch, T., Davidovits, P., Worsnop, D., and Knopf, D.: The deposition ice nucleation and immersion freezing potential of amorphous secondary organic aerosol: pathways for ice and mixed-phase cloud formation, J. Geophys. Res., 117, D16209, doi:10.1029/2012JD017446, 2012. 7813

Wang, P., Grover, S., and Pruppacher, H.: On the effect of electric charges on the scavenging of aerosol particles by clouds and small raindrops, J. Atmos. Sci., 35, 1735–1743, 1978. 7814, 7818, 7819

Wieringa, J. and Holleman, I.: If cannons cannot fight hail, what else?, Meteorol. Z., 15, 659–669, 2006. 7813

Wise, M. E., Baustian, K. J., Koop, T., Freedman, M. A., Jensen, E. J., and Tolbert, M. A.: Depositional ice nucleation onto crystalline hydrated NaCl particles: a new mechanism for ice formation in the troposphere, Atmos. Chem. Phys., 12, 1121–1134, doi:10.5194/acp-12-1121-2012, 2012. 7813

Young, K.: The role of contact nucleation in ice phase initiation in clouds, J. Atmos. Sci., 31, 768–776, 1974a. 7818

Young, K.: A numerical simulation of wintertime, orographic precipitation, Part 1: Description of model microphysics and numerical techniques, J. Atmos. Sci., 31, 1735–1748, 1974b. 7838

Zardini, A., Krieger, U., and Marcolli, C.: White light Mie resonance spectroscopy used to measure very low vapor pressures of substances in aqueous solution aerosol particles, Opt. Express, 14, 6951–6962, 2006. 7861

ACPD
13, 7811–7869, 2013

Table 1. Literature review of experimental studies on contact freezing using different instrumentation and aerosol particles. [AP] means aerosol particle concentration, PG phloroglucinol, DN 1-5-dihydroxynaphthalene and MA metaldehyde.

Authors	Instrument	IN composition	Drop radii (μm)	aerosol radii (μm)	Polydisperse AP	Monodisperse AP	[AP] control	RH control
Gokhale and Goold Jr. (1968)	cold plate	AgI, clay, CuS, volcanic ash	1350	0.025–200	X			
Gokhale and Lewinter (1971)	cold plate	AgI	1000	> 1	X			
Gokhale and Spengler (1972)	wind tunnel	AgI, clay, NaCl, sand	2000–3000	1.4, 1.6	X			
Fletcher (1972)	cold plate	100 different organic compounds	1500–2500	unknown				
Sax and Goldsmith (1972)	drop-freezing apparatus	AgI, CuI, and Ag_2O	20–80	0.01		X		
Pitter and Pruppacher (1973)	wind tunnel	kaolinite, montmorillonite	325	0.05–15	X			
Fukuta (1975)	cold plate	DN, MA and PG	500	unknown				
Rosinski and Nagamoto (1976)	cold plate/ cold chamber	two soil samples	1000	0.5–25	X			
Langer et al. (1978)	NCAR ice nucleus counter	AgI and DN	3 (median size)	0.01–0.06	X	X		
Schaller and Fukuta (1979)	thermal diffusion chamber	AgI, DN, MA and PG	unknow	< 0.3		X		
Levin and Yankofsky (1983)	wind tunnel	Bacteria	220–360	< 0.23	X			
DeMott et al. (1983)	isothermal cloud chamber	AgI, AgI-Cl	1–8	0.005–0.14	X			
Deshler and Vali (1992)	sampling apparatus	AgI and natural aerosols	1300	0.005–0.1	X			
DeMott (1995)	isothermal cloud chamber	AgI-AgCl	1–8	0.015, 0.026, 0.035		X		
Diehl and Mitra (1998)	wind tunnel	kerosene	170–410	0.045–0.1	X			
Diehl et al. (2002)	wind tunnel	pollen	360	12.5–35	X			
Shaw et al. (2005)	cold plate	volcanic ash	≈ 1900	50–150		X		
Durant and Shaw (2005)	cold plate	volcanic ash, soda glass	≈ 1500–2000	200–325 115		X	X	
Von Blohn et al. (2005)	wind tunnel	pollen	315–380	13–14	X		X	
Fornea et al. (2009)	cold plate	volcanic ash	≈ 782	125–150		X		
Svensson et al. (2009)	EDB	kaolinite	25	0.15–2.5	X		X	X
Ladino et al. (2011b)	CLINCH	kaolinite	12.5	0.2, 0.4		X	X	X (100 % RHi)
Bunker et al. (2012)	cold plate	kaolinite and ATD	≈ 1060	0.063–1.0		X	X	

ACPD
13, 7811–7869, 2013

Table 2. Summary of the freezing temperatures for contact and immersion freezing conducted on a cold plate. $\widetilde{T}$ is the average onset freezing temperature (temperature at which the tested drops freeze) for contact freezing (CF), immersion freezing (IF) and homogeneous freezing (HF), respectively.

Authors	IN composition	$\widetilde{T}$ for CF (K)	$\widetilde{T}$ for IF (K)	$\widetilde{T}$ for HF (K)
Gokhale and Goold Jr. (1968)	AgI,Clay, CuS, volcanic ash	267	–	265
Gokhale and Lewinter (1971)	AgI	267	–	–
Fukuta (1975)	1–5dihydroxynaphthalene	266	–	–
Fukuta (1975)	metaldehyde	270	–	–
Fukuta (1975)	phloroglucinol	267	–	–
Rosinski and Nagamoto (1976)	two soil samples	268	–	–
Shaw et al. (2005)	volcanic ash	254–255	251	246–247
Durant and Shaw (2005)	glass-rich volcanic ash	256	252	–
Durant and Shaw (2005)	soda glass	255	252	–
Fornea et al. (2009)	Mount St. Helens Ash	262	255	–
Fornea et al. (2009)	IHSS Pahokee Peat Soil II	263	–	–
Fornea et al. (2009)	Carbon (Lampblack)	248	–	–

ACPD
13, 7811–7869, 2013

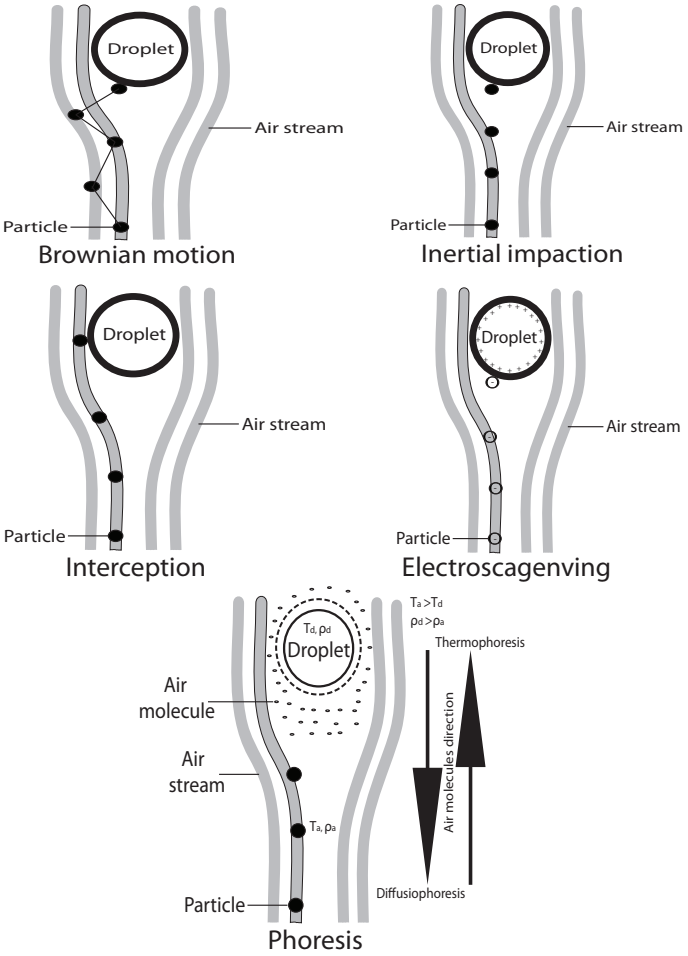

Fig. 1. Diagram of the different collisions pathways between aerosol particles and cloud droplets relevant to contact freezing (Ladino, 2011).

ACPD
13, 7811–7869, 2013

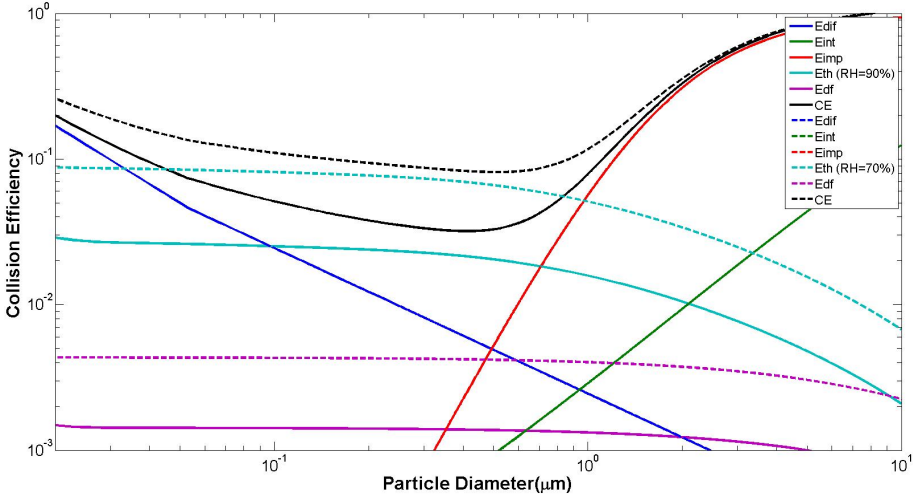

Fig. 2. Theoretical collision efficiency as a function of aerosol radius for a cloud droplet with a radius of 12.8 μm and the contribution of each single force. E_{dif}, E_{int}, E_{imp}, E_{Th} and E_{Df} are the collision efficiency due to Brownian motion, interception, inertial impaction, thermophoresis and diffusiophoresis respectively. CE is the total collision efficiency. E_{Th}, E_{Df} and hence CE have been calculated for a relative humidity (RH_w) of 90 % (solid lines) and for RH_w = 70 % (dashed lines).

ACPD
13, 7811–7869, 2013

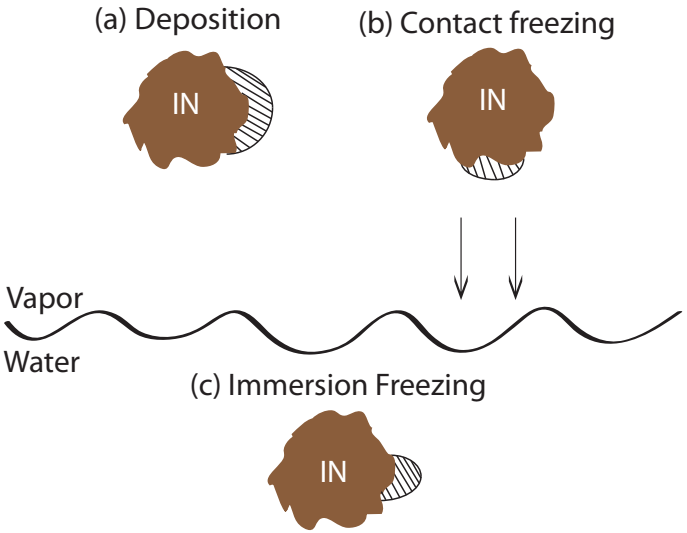

Fig. 3. Illustration of nucleation mechanisms, and the critical embryo sizes (shaded areas) required for nucleation (Cooper, 1974).

ACPD
13, 7811–7869, 2013

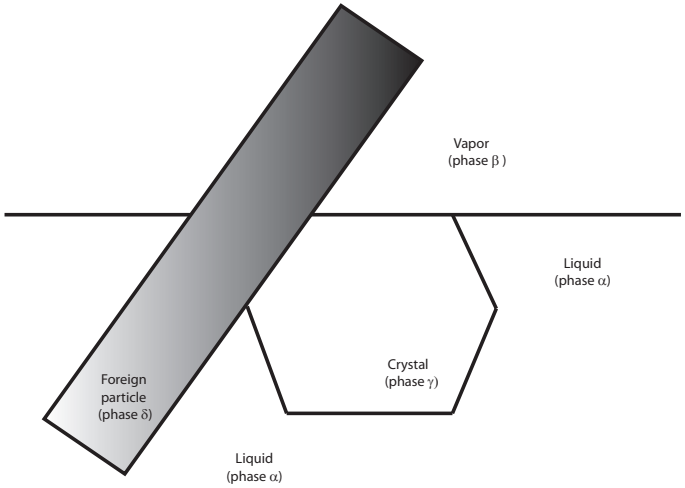

Fig. 4. Mechanism of contact freezing based on the different phases interactions (Djikaev and Ruckenstein, 2008).

ACPD
13, 7811–7869, 2013

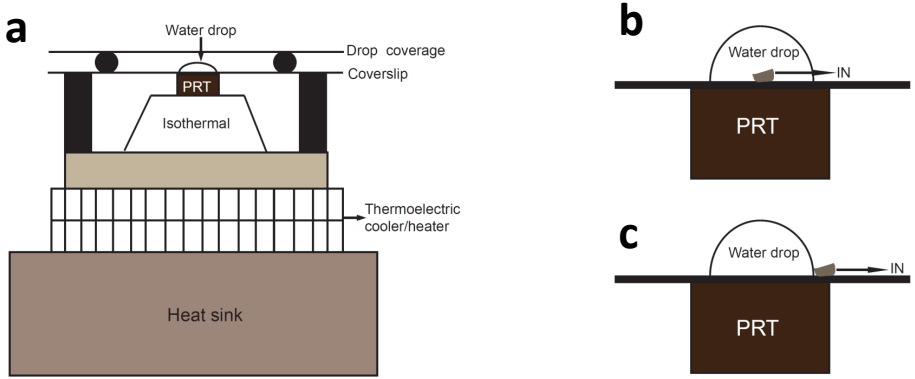

Fig. 5. (a) Schematic with the cold plate experimental setup (left). **(b)** Location of the IN for an immersion freezing (top right) and **(c)** for a contact freezing experiment (bottom right) (Shaw et al., 2005).

ACPD
13, 7811–7869, 2013

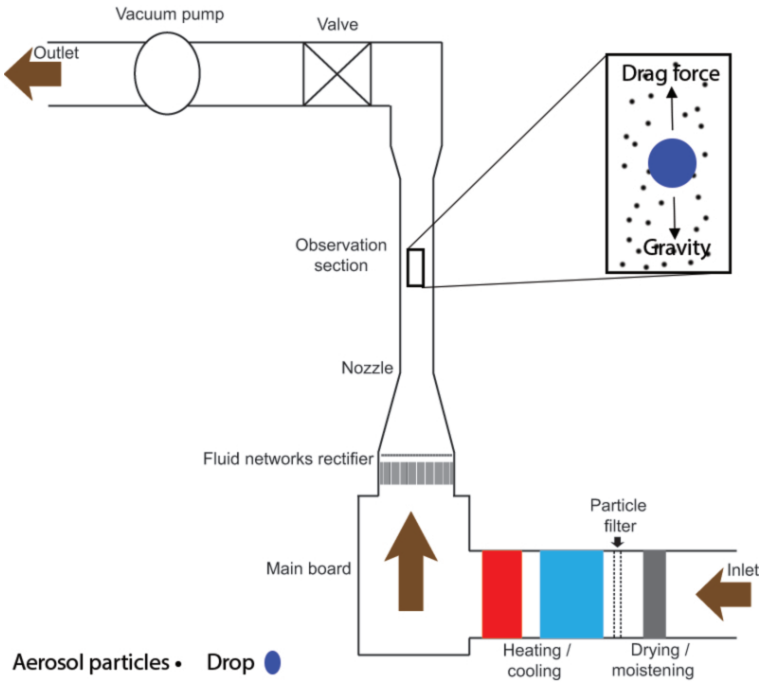

Fig. 6. Schematic of the wind tunnel experimental setup and its major components (Vohl et al., 1999).

ACPD
13, 7811–7869, 2013

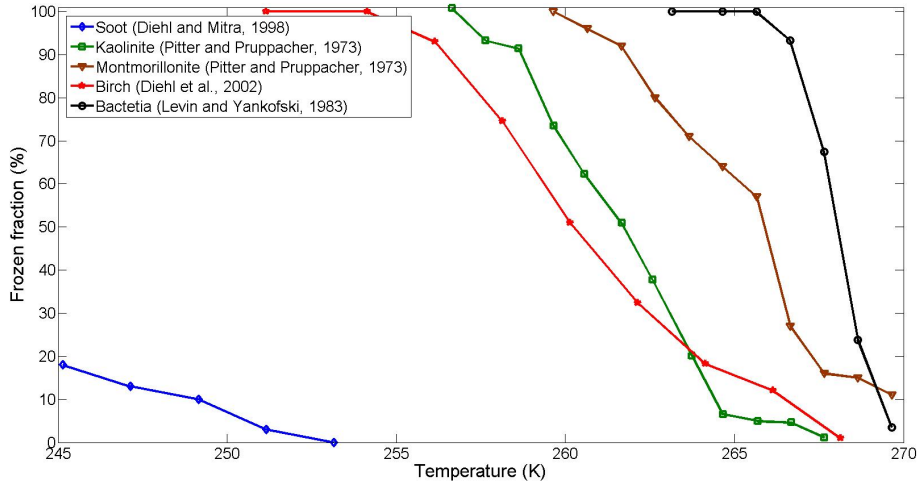

Fig. 7. Comparison of different contact freezing experiments conducted in a wind tunnel. The blue color represent the experiments done with soot particles, green with kaolinite, brown with montmorillonite, red with pollen and black with bacteria (Pitter and Pruppacher, 1973; Levin and Yankofsky, 1983; Diehl and Mitra, 1998; Diehl et al., 2002).

ACPD
13, 7811–7869, 2013

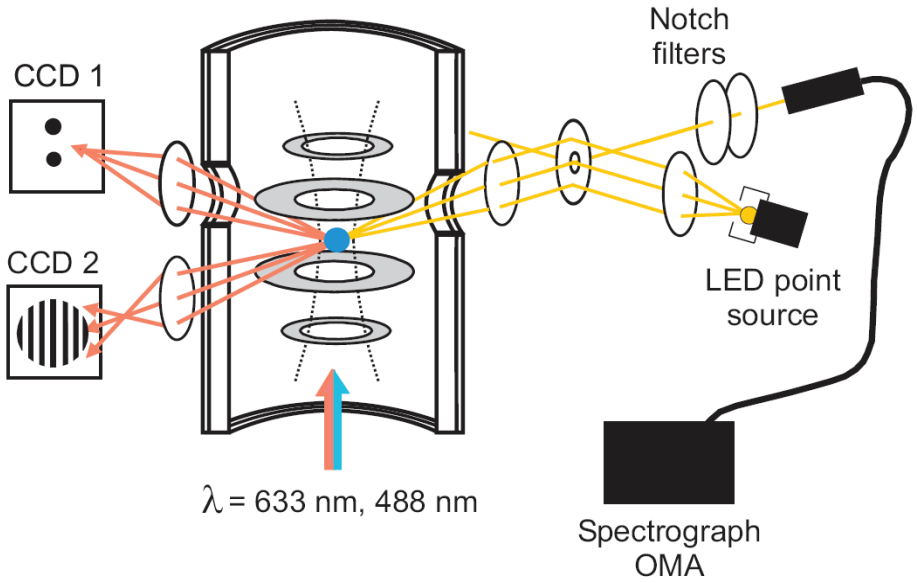

Fig. 8. Schematic with the electrodynamic balance experimental setup (Duft and Leisner, 2004a; Zardini et al., 2006).

ACPD
13, 7811–7869, 2013

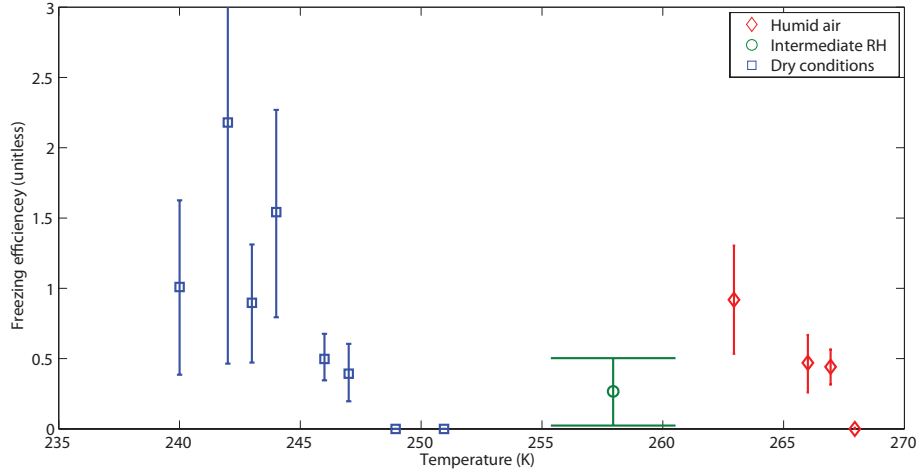

Fig. 9. Freezing efficiencies of kaolinite particles obtained in an EDB. Red, green and blue colors represent the experiments at high, intermediate and low relative humidity with respect to water (Svensson et al., 2009).

ACPD
13, 7811–7869, 2013

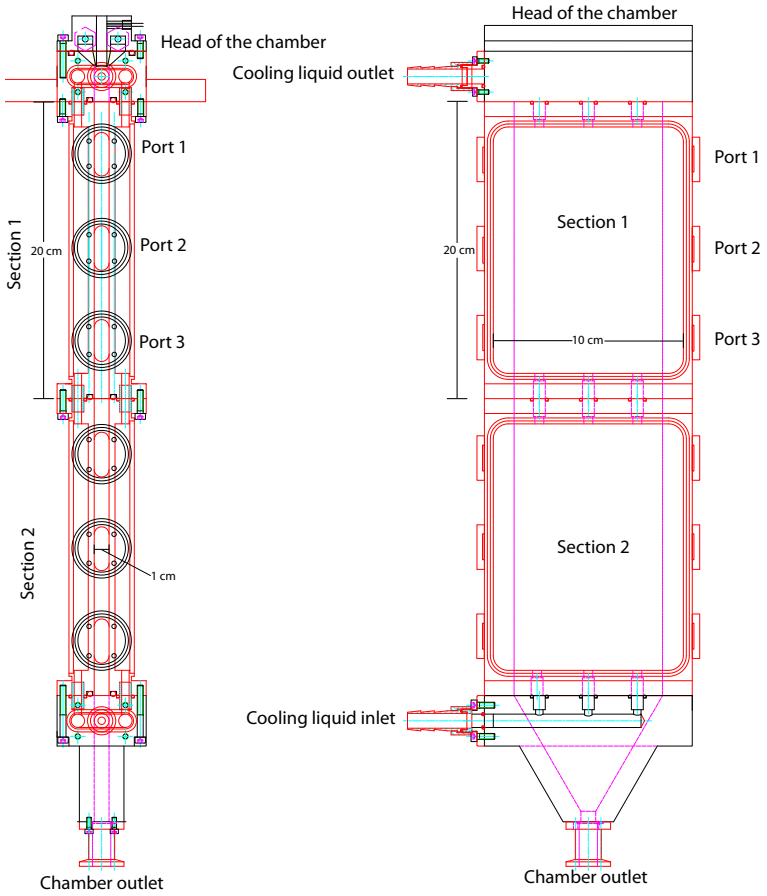

Fig. 10. Schematic with the CLINCH experimental setup. (left) side view and (right) front view of the instrument (Ladino, 2011).

ACPD
13, 7811–7869, 2013

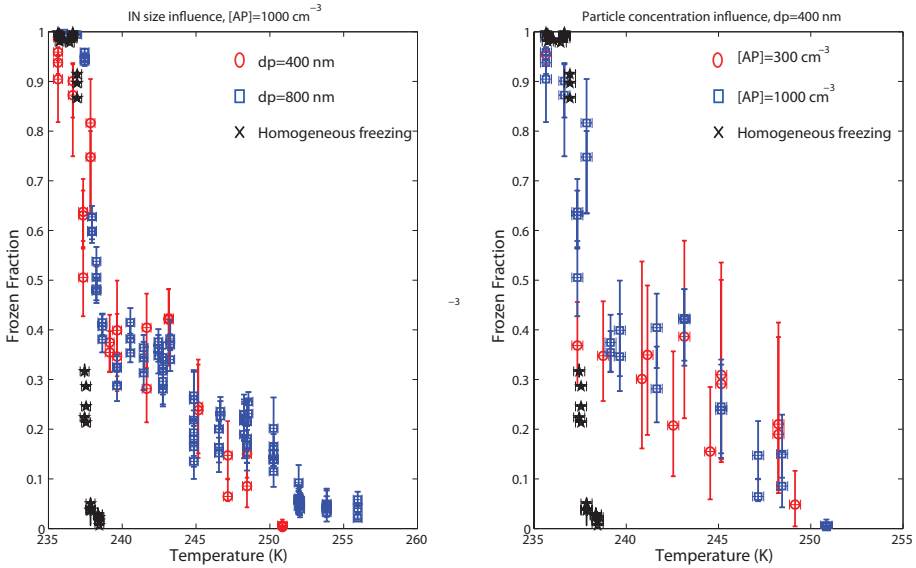

Fig. 11. Experimental frozen fraction on contact freezing as a function of temperature conducted in CLINCH. The cloud droplets have a residence time of 5 s. The left panel shows the comparison of two different particle sizes and the right panel the comparison of two different aerosol particle concentrations. The black starts represent the homogeneous freezing data. dp refers to the aerosol particle diameter and [AP] to the aerosol particle concentration.

ACPD
13, 7811–7869, 2013

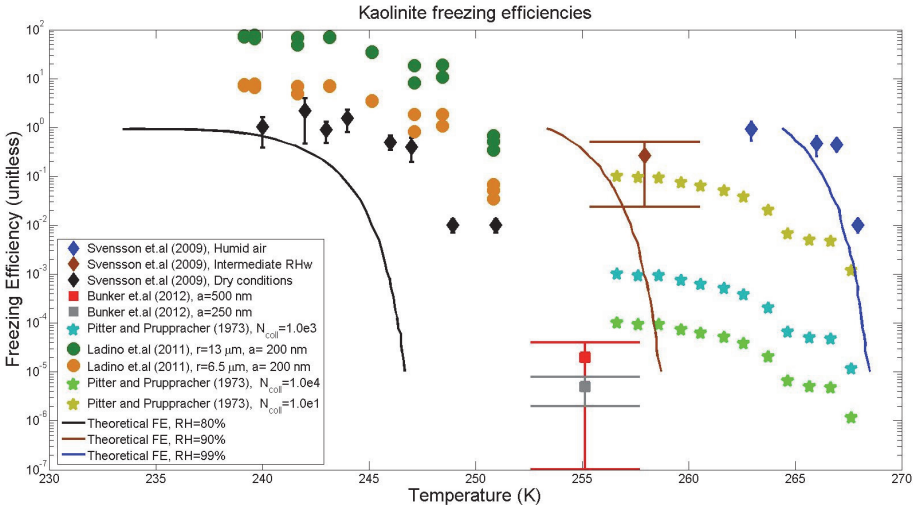

Fig. 12. Comparison of the available kaolinte freezing efficiences due to contact nucleation as a function of temperature from different instrumentation. In those studies who reported frozen fractions we have calculated the freezing efficiency assuming different values for N_{coll}. The stars represent the wind tunnel data with different assumptions for the unknown parameter N_{coll} (Pitter and Pruppacher, 1973), whereas the diamonds, circles and squares the data from the EDB (Svensson et al., 2009), CLINCH (Ladino et al., 2011b) and the cold plate data (Bunker et al., 2012), respectively.

ACPD
13, 7811–7869, 2013

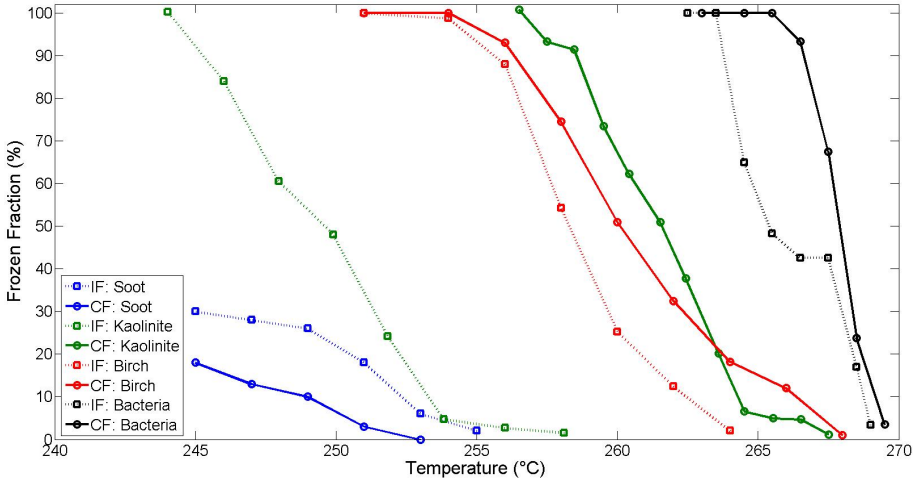

Fig. 13. Comparison of contact freezing (CF) and immersion freezing (IF) results as a function of temperature using different IN's. All the experiments were conducted in a wind tunnel. The contact freezing and the immersion freezing experiments are represented by the solid (circles) and dotted (squares) lines respectively. The blue color represent the experiments done with soot particles, green with kaolinite, red with pollen and black with bacteria (Pitter and Pruppacher, 1973; Levin and Yankofsky, 1983; Diehl and Mitra, 1998; Diehl et al., 2002). Note that the collision rates are not accounted in any of the presented results.

ACPD
13, 7811–7869, 2013

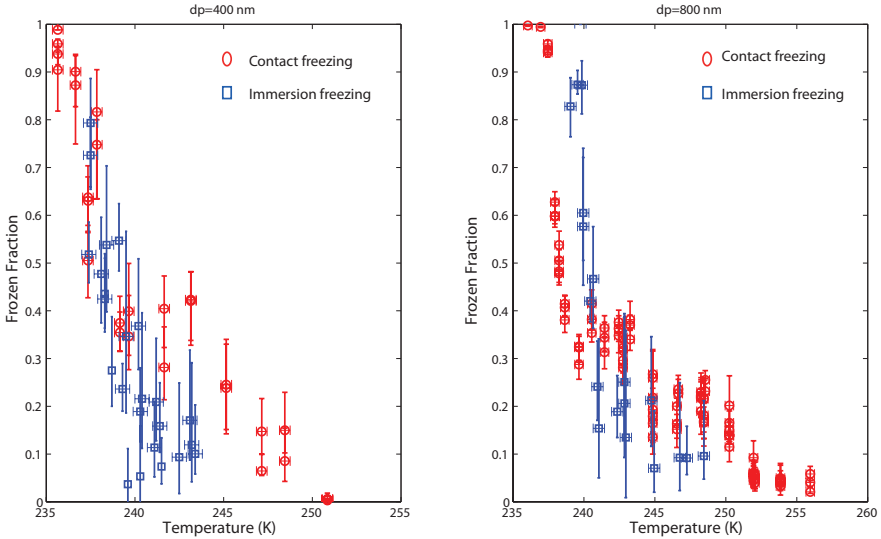

Fig. 14. Comparison of contact freezing and immersion freezing results for kaolinite particles. Red circles represent the contact freezing experiments for cloud droplet of 26 µm (in diameter) with a residence time of 5 s, whereas the blue squares the immersion freezing data with a droplet diameter of 6 µm. dp refers to the aerosol particle diameter.

ACPD
13, 7811–7869, 2013

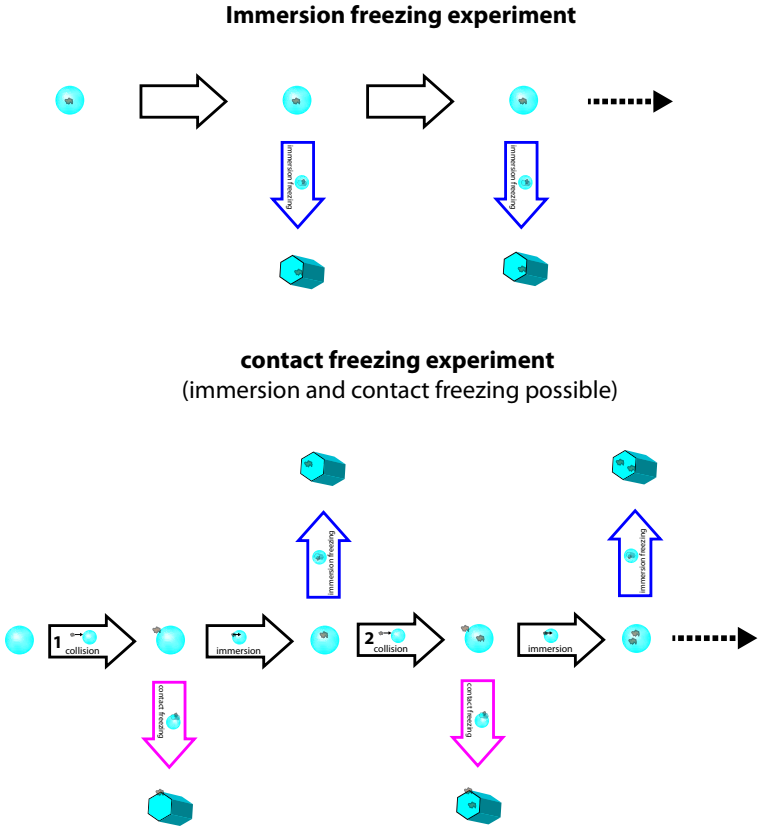

Fig. 15. Schematic of a typical contact and immersion freezing experiment. For details refer to the main text.

ACPD
13, 7811–7869, 2013

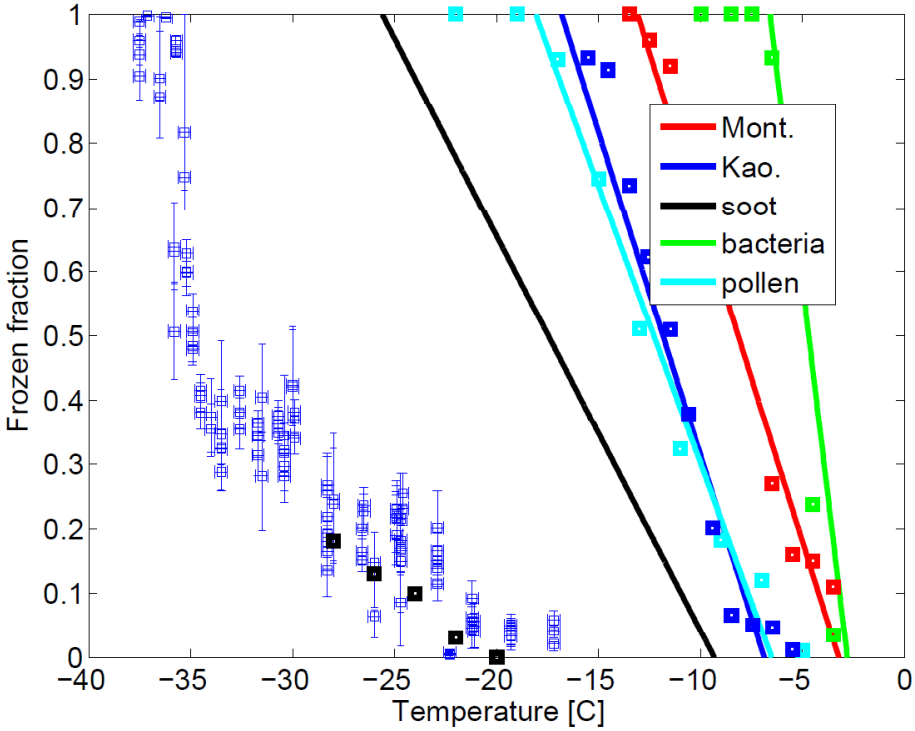

Fig. 16. Comparison of frozen fractions obtained from wind tunnel studies (thick squares) using kaolinite and montmorillonite (Pitter and Pruppacher, 1973), soot (Diehl and Mitra, 1998), pollen (Diehl et al., 2002) and bacteria (Levin and Yankofsky, 1983) and CLINCH (thin squares with error bars) using kaolinite (Ladino et al., 2011b) as compared with the parameterized frozen fractions by Diehl et al. (2006).

ACPD
13, 7811–7869, 2013